Local Multigrid in $\mathbf{H}(\mathbf{curl})$

R. Hiptmair and W. Zheng[1]

Research Report No. 2007-03
February 2007
Seminar für Angewandte Mathematik
Eidgenössische Technische Hochschule
CH-8092 Zürich
Switzerland

[1]LSEC, Institute of Computational Mathematics, Academy of Mathematics and System Sciences, Chinese Academy of Sciences, Beijing, 100080, People's Republic of China. This author was supported in part by China NSF under the grant 10401040 (zwy@lsec.cc.ac.cn).

Local Multigrid in $\boldsymbol{H}(\mathbf{curl})$

R. Hiptmair and W. Zheng[1]

Seminar für Angewandte Mathematik
Eidgenössische Technische Hochschule
CH-8092 Zürich
Switzerland

Research Report No. 2007-03 February 2007

Abstract

We consider $\boldsymbol{H}(\mathbf{curl}, \Omega)$-elliptic variational problems on bounded Lipschitz polyhedra and their finite element Galerkin discretization by means of lowest order edge elements. We assume that the underlying tetrahedral mesh has been created by successive local mesh refinement, either by local uniform refinement with hanging nodes or bisection refinement. In this setting we develop a convergence theory for the the so-called local multigrid correction scheme with hybrid smoothing. We establish that its convergence rate is uniform with respect to the number of refinement steps. The proof relies on corresponding results for local multigrid in a $H^1(\Omega)$-context along with local discrete Helmholtz-type decompositions of the edge element space.

Keywords: Edge elements, local multigrid, stable multilevel splittings, subspace correction theory, regular decompositions of $\boldsymbol{H}(\mathbf{curl})$, Helmholtz-type decompositions

AMS Subject Classification: 65N30, 65N55, 78A25

[1]LSEC, Institute of Computational Mathematics, Academy of Mathematics and System Sciences, Chinese Academy of Sciences, Beijing, 100080, People's Republic of China. This author was supported in part by China NSF under the grant 10401040 (zwy@lsec.cc.ac.cn).

1. Introduction. On a polyhedron Ω, scaled such that $\operatorname{diam}(\Omega) = 1$, we consider the variational problem: seek $\mathbf{u} \in \boldsymbol{H}_{\Gamma_D}(\mathbf{curl}, \Omega)$ such that

$$\underbrace{(\mathbf{curl}\,\mathbf{u}, \mathbf{curl}\,\mathbf{v})_{L^2(\Omega)} + (\mathbf{u}, \mathbf{v})_{L^2(\Omega)}}_{=:\mathsf{a}(\mathbf{u},\mathbf{v})} = (\mathbf{f}, \mathbf{v})_{L^2(\Omega)} \quad \forall \mathbf{v} \in \boldsymbol{H}_{\Gamma_D}(\mathbf{curl}, \Omega)\ . \tag{1.1}$$

For the Hilbert space of square integrable vector fields with square integrable **curl** and vanishing tangential components on Γ_D we use the symbol $\boldsymbol{H}_{\Gamma_D}(\mathbf{curl}, \Omega)$, see [20, Ch. 1] for details. The source term $\mathbf{f}$ in (1.1) is a vector field in $(L^2(\Omega))^3$. The left hand side of (1.1) agrees with the inner product of $\boldsymbol{H}_{\Gamma_D}(\mathbf{curl}, \Omega)$ and will be abbreviated by $\mathsf{a}(\mathbf{u}, \mathbf{v})$ ("energy inner product").

Further, Γ_D denotes the part of the boundary $\partial\Omega$ on which homogeneous Dirichlet boundary conditions in the form of vanishing tangential traces of $\mathbf{u}$ are imposed. The geometry of the Dirichlet boundary part Γ_D is supposed to be simple in the following sense: for each connected component Γ_i of Γ_D we can find an open Lipschitz domain $\Omega_i \subset \mathbb{R}^3$ such that

$$\overline{\Omega}_i \cap \overline{\Omega} = \Gamma_i\ , \quad \Omega_i \cap \Omega = \emptyset\ , \tag{1.2}$$

and Ω_i and Ω_j have positive distance for $i \neq j$. Further, the interior of $\overline{\Omega} \cup \overline{\Omega_1} \cup \overline{\Omega_2} \ldots$ is expected to be a Lipschitz-domain, too (see Fig. 5.2). This is not a severe restriction, because variational problems related to (1.1) usually arise in quasi-static electromagnetic modelling, where simple geometries are common. Of course, $\Gamma_D = \emptyset$ is admitted.

Lowest order $\boldsymbol{H}_{\Gamma_D}(\mathbf{curl}, \Omega)$-conforming edge elements are widely used for the finite element Galerkin discretization of variational problems like (1.1). Then, for sufficiently smooth solution $\mathbf{u}$ we can expect the optimal asymptotic convergence rate

$$\|\mathbf{u} - \mathbf{u}_h\|_{\boldsymbol{H}(\mathbf{curl},\Omega)} \leq C N_h^{-1/3}\ , \tag{1.3}$$

on families of finite element meshes arising from global refinement. Here, $\mathbf{u}_h$ is the finite element solution, and N_h the dimension of the finite element space. However, often $\mathbf{u}$ will fail to possess the required regularity due to singularities arising at edges/corners of $\partial\Omega$ and material interfaces [18,19]. Fortunately, it seems to be possible to retain (1.3) by the use of adaptive local mesh refinement based on a posteriori error estimates, see [6,14] for numerical evidence.

We also need ways to *compute* the asymptotically optimal finite element solution with optimal computational effort, that is, with a number of operations proportional to N_h, *cf.* [42]. This can only be achieved by means of iterative solvers, whose convergence remains fast regardless of the depth of refinement. Multigrid methods are the most prominent class of iterative solvers that achieve this goal. By now, multigrid methods for discrete $\boldsymbol{H}(\mathbf{curl}, \Omega)$-elliptic variational problems like (1.1) have become well established [16, 24, 41, 43]. Their asymptotic theory on sequencies of regularly refined meshes has also matured [2, 21, 24, 26]. It confirms *asymptotic optimality*: the speed of convergence is uniformly fast regardless of the number of refinement levels involved. In addition, the costs of one step of the iteration scale linearly with the number of unknowns.

Yet, the latter property is lost when the standard multigrid correction scheme is applied to meshes generated by pronounced local refinement. Optimal computational costs can only be maintained, if one adopts the local multigrid policy, which was pioneered by W. Mitchell in [32]. Crudely speaking, its gist is to confine relaxations to "new" degrees of freedom located in zones where refinement has changed the mesh. Thus an exponential increase of computational costs with the number of refinement level can be avoided: the total costs of a V-cycle remain proportional to the number of unknowns. Algorithmically, it is straightforward to apply the local multigrid idea to lowest-order edge element approximations of (1.1). On the other hand, a proof of uniform asymptotic convergence has remained elusive so far. It is the objective of this paper to provide it.

It is an important insight, that (1.1) is one member of a family of variational problems. Its kin is obtained by replacing **curl** with grad or div, respectively. All these differential operators turn out to be incarnations of the fundamental exterior derivative of differential geometry, *cf.* [24, Sect. 2]. They are closely connected in the deRham complex [3] and, thus, it is hardly surprising that results about the related $H^1_{\Gamma_D}(\Omega)$-elliptic variational problem, which seeks $u \in H^1_{\Gamma_D}(\Omega)$ such that

$$(1.4) \qquad (\operatorname{grad} u, \operatorname{grad} v)_{L^2(\Omega)} + (u, v)_{L^2(\Omega)} = (f, v)_{L^2(\Omega)} \quad \forall\, v \in H^1_{\Gamma_D}(\Omega)\ ,$$

prove instrumental in the multigrid analysis for discretized versions of (1.1). Here $H^1_{\Gamma_D}(\Omega)$ is the subspace of $H^1(\Omega)$ whose functions have vanishing traces on Γ_D.

Thus, when tackling (1.1), we take the cue from the local multigrid theory for (1.4) discretized by means of linear continuous finite elements. This theory has been developed in various settings, *cf.* [4, 9, 11, 12, 47]. In [1] local refinement with hanging nodes is treated. Recently, H. Wu and Z. Chen [14] proved the uniform convergence of V-cycle multigrid method on adaptively refined meshes. Their mesh refinements are controlled by a posteriori error estimators and the "newest vertex bisection" strategy introduced in [5] and [32]. As in the case of global multigrid, the essential new aspect of local multigrid theory for (1.1) compared to (1.4) is the need to deal with the kernel of the **curl**-operator, *cf.* [24, Sect. 3]. Here, the capability of edge elements to provide a simple representation of discrete irrotational vector fields becomes pivotal.

Therefore, we devote the entire Sect. 2 to the discussion of edge elements and their relationship with conventional Lagrangian finite elements. Next, in Sect. 3 we present details about local mesh refinement, because some parts of the proofs rest on the subtleties of how elements are split. The following Sect. 4 introduces the local multigrid method from the abstract perspective of successive subspace correction.

The proof of uniform convergence (Theorem 4.2) is tackled in Sects. 5 and 6, which form the core of the article. In particular, the investigation of the stability of the local multilevel splitting requires several steps, the first of which addresses the issue for the bilinear form from (1.4) and linear finite elements. These results are already available in the literature, but are re-derived to make the presentation self-contained. This also applies to the continuous and discrete Helmholtz-type decompositions covered in Sect. 5.3. Eventually, in Sect. 7, we report two numerical experiments to show the competitive performance of the local multigrid method and the relevance of the convergence theory.

2. Finite element spaces. Whenever we refer to a finite element mesh in this article, we have in mind a tetrahedral triangulation of Ω, see [15, Ch. 3]. In certain settings, it may feature hanging nodes, that is, the face of one tetrahedron can coincide with the union of faces of other tetrahedra. Further, the mesh is supposed to resolve the Dirichlet boundary in the sense that Γ_D is the union of faces of tetrahedra. The symbol $\mathcal{M}$ with optional subscripts is reserved for finite element meshes and the sets of their elements alike.

We write $h \in L^\infty(\Omega)$ for the piecewise constant function, which assumes value $h_K := \mathrm{diam}(K)$ in each element $K \in \mathcal{M}$. The ratio of $\mathrm{diam}(K)$ to the radius of the largest ball contained in K is called the shape regularity measure ρ_K [15, Ch. 3, §3.1]. The shape regularity measure $\rho_{\mathcal{M}}$ of $\mathcal{M}$ is the maximum of all ρ_K, $K \in \mathcal{M}$.

Based on a finite element mesh $\mathcal{M}$ we introduce the space of lowest order $\boldsymbol{H}_{\Gamma_D}(\mathbf{curl}, \Omega)$-conforming edge finite elements [10, 33], also known as Whitney-1-forms [44],

$$\mathbf{U}(\mathcal{M}) := \{\mathbf{v}_h \in \boldsymbol{H}_{\Gamma_D}(\mathbf{curl}, \Omega) : \ \forall K \in \mathcal{M} : \exists\, \boldsymbol{a}, \boldsymbol{b} \in \mathbb{R}^3 : \\ \mathbf{v}_h(\boldsymbol{x}) = \boldsymbol{a} + \boldsymbol{b} \times \boldsymbol{x},\ \boldsymbol{x} \in K\} \ .$$

For a detailed derivation and description please consult [25, Sect. 3]. Notice that $\mathbf{curl}\,\mathbf{U}(\mathcal{M})$ is a space of piecewise constant vector fields. We also remark that appropriate global degrees of freedom (d.o.f.) for $\mathbf{U}(\mathcal{M})$ are given by

$$\left\{ \begin{array}{rcl} \mathbf{U}(\mathcal{M}) & \mapsto & \mathbb{R} \\ \mathbf{v}_h & \mapsto & \int_E \mathbf{v}_h \cdot \mathrm{d}\vec{s} \end{array} \right. \quad , \quad E \in \mathcal{E}(\mathcal{M}) \ , \tag{2.1}$$

where $\mathcal{E}(\mathcal{M})$ is the set of active edges of $\mathcal{M}$, *i.e.*, those not contained in Γ_D or in another longer edge. We write $\mathfrak{B}_{\mathbf{U}}(\mathcal{M})$ for the nodal basis of $\mathbf{U}(\mathcal{M})$ dual to the global d.o.f. (2.1). Basis functions are associated with active edges. Hence, we can write $\mathfrak{B}_{\mathbf{U}}(\mathcal{M}) = \{\mathbf{b}_E\}_{E \in \mathcal{E}(\mathcal{M})}$. In the absence of hanging nodes the support of the basis function $\mathbf{b}_E$ is the union of tetrahedra sharing the edge E. We recall the simple formula for local shape functions

$$\mathbf{b}_{E|K} = \lambda_i \,\mathrm{grad}\, \lambda_j - \lambda_j \,\mathrm{grad}\, \lambda_i \quad E = [\boldsymbol{a}_i, \boldsymbol{a}_j] \subset \overline{K} \tag{2.2}$$

for any tetrahedron $K \in \mathcal{M}$ with vertices $\boldsymbol{a}_i$, $i = 1, 2, 3, 4$, and associated barycentric coordinate functions λ_i.

The edge element space $\mathbf{U}(\mathcal{M})$ with basis $\mathfrak{B}_{\mathbf{U}}(\mathcal{M})$ is perfectly suited for the finite element Galerkin discretization of (1.1). The discrete problem based on $\mathbf{U}(\mathcal{M})$ reads: seek $\mathbf{u}_h \in \mathbf{U}(\mathcal{M})$ such that

$$(\mathbf{curl}\,\mathbf{u}_h, \mathbf{curl}\,\mathbf{v}_h)_{L^2(\Omega)} + (\mathbf{u}_h, \mathbf{v}_h)_{L^2(\Omega)} = (\mathbf{f}, \mathbf{v}_h)_{L^2(\Omega)} \quad \forall \mathbf{v}_h \in \mathbf{U}(\mathcal{M}) \ . \tag{2.3}$$

The properties of $\mathbf{U}(\mathcal{M})$ will be key to constructing and analyzing the local multigrid method for the resulting large sparse linear system of equations. Next, we collect important facts.

The basis $\mathfrak{B}_{\mathbf{U}}(\mathcal{M})$ enjoys uniform L^2-stability, meaning the existence of a constant $C = C(\rho_{\mathcal{M}}) > 0$ such that for all $\mathbf{v}_h = \sum\limits_{E \in \mathcal{E}(\mathcal{M})} \alpha_E \mathbf{b}_E \in \mathbf{U}(\mathcal{M})$, $\alpha_E \in \mathbb{R}$,

$$C^{-1} \left\| \mathbf{v}_h \right\|^2_{L^2(\Omega)} \le \sum_{E \in \mathcal{E}(\mathcal{M})} \alpha_E^2 \left\| \mathbf{b}_E \right\|^2_{L^2(\Omega)} \le C \left\| \mathbf{v}_h \right\|^2_{L^2(\Omega)} \ . \tag{2.4}$$

The global d.o.f. induce a nodal edge interpolation operator

$$\boldsymbol{\Pi}_h : \left\{ \begin{array}{rcl} \mathrm{dom}(\boldsymbol{\Pi}_h) \subset \boldsymbol{H}_{\Gamma_D}(\mathbf{curl}, \Omega) & \mapsto & \mathbf{U}(\mathcal{M}) \\ \mathbf{v} & \mapsto & \sum\limits_{E \in \mathcal{E}(\mathcal{M})} \left(\int_E \mathbf{v} \cdot \mathrm{d}\vec{s} \right) \cdot \mathbf{b}_E \ . \end{array} \right. \tag{2.5}$$

Obviously, $\mathbf{\Pi}_h$ provides a local projection, but it turns out to be unbounded even on $(H^1(\Omega))^3$. Only for vector fields with discrete rotation the following interpolation error estimate is available, see [25, Lemma 4.6]:

LEMMA 2.1. *The interpolation operator* $\mathbf{\Pi}_h$ *is bounded on* $\{\mathbf{\Psi} \in (H^1(\Omega))^3, \mathbf{curl}\,\mathbf{v} \in \mathbf{curl}\,\mathbf{U}(\mathcal{M})\}$, *and for any* conforming *mesh there is* $C = C(\rho_\mathcal{M}) > 0$ *such that*

$$\left\| h^{-1}(Id - \mathbf{\Pi}_h)\mathbf{\Psi} \right\|_{L^2(\Omega)} \leq C|\mathbf{\Psi}|_{H^1(\Omega)} \quad \forall \mathbf{\Psi} \in (H^1(\Omega))^3,\ \mathbf{curl}\,\mathbf{\Psi} \in \mathbf{curl}\,\mathbf{U}(\mathcal{M})\ .$$

If Ω is homeomorphic to a ball, then $\operatorname{grad} H^1(\Omega) = \boldsymbol{H}(\mathbf{curl}\,0, \Omega) := \{\mathbf{v} \in \boldsymbol{H}(\mathbf{curl}, \Omega), \mathbf{curl}\,\mathbf{v} = 0\}$: $H^1(\Omega)$ provides scalar potentials for $\boldsymbol{H}(\mathbf{curl}, \Omega)$. To state a discrete analogue of this relationship we need the Lagrangian finite element space of piecewise linear continuous functions on $\mathcal{M}$

$$V(\mathcal{M}) := \{u_h \in H^1_{\Gamma_D}(\Omega) :\ u_{h|K} \in \mathbb{P}_1(K)\ \forall K \in \mathcal{M}\}\ ,$$

where $\mathbb{P}_p(K)$ is the space of 3-variate polynomials of degree $\leq p$ on K. The global degrees of freedom for $V(\mathcal{M})$ boil down to point evaluations at active vertices (set $\mathcal{N}(\mathcal{M})$) of $\mathcal{M}$. The dual basis of "tent functions" will be denoted by $\mathfrak{B}_V(\mathcal{M}) = \{b_{\boldsymbol{p}}\}_{\boldsymbol{p} \in \mathcal{N}(\mathcal{M})}$. Its unconditional L^2-stability is well known: with a universal constant $C > 0$ we have for all $u_h = \sum_{\boldsymbol{p} \in \mathcal{N}(\mathcal{M})} \alpha_{\boldsymbol{p}} b_{\boldsymbol{p}} \in V(\mathcal{M})$, $\alpha_{\boldsymbol{p}} \in \mathbb{R}$,

$$C^{-1} \left\| u_h \right\|^2_{L^2(\Omega)} \leq \sum_{\boldsymbol{p} \in \mathcal{N}(\mathcal{M})} \alpha^2_{\boldsymbol{p}} \left\| b_{\boldsymbol{p}} \right\|^2_{L^2(\Omega)} \leq C \left\| u_h \right\|^2_{L^2(\Omega)}\ . \tag{2.6}$$

For the nodal interpolation operator related to $\mathfrak{B}_V$ we write $\mathcal{I}_h : \operatorname{dom}(\mathcal{I}_h) \subset H^1_{\Gamma_D}(\Omega) \mapsto V(\mathcal{M})$. Recall the standard estimate for linear interpolation on *conforming* meshes (i.e., no hanging nodes allowed) that asserts the existence of $C = C(k, \rho_\mathcal{M}) > 0$ such that

$$\left\| h^{k-2}(Id - \mathcal{I}_h)u \right\|_{H^k(\Omega)} \leq C|u|_{H^2(\Omega)} \quad \forall u \in H^2(\Omega) \cap H^1_{\Gamma_D}(\Omega),\ k \in \{0, 1, 2\}\ . \tag{2.7}$$

Obviously, $\operatorname{grad} V(\mathcal{M}) \subset \mathbf{U}(\mathcal{M})$, and immediate from Stokes theorem is the crucial *commuting diagram property*

$$\mathbf{\Pi}_h \circ \operatorname{grad} = \operatorname{grad} \circ \mathcal{I}_h \quad \text{on } \operatorname{dom}(\mathcal{I}_h)\ . \tag{2.8}$$

This enables us to give an elementary proof of Lemma 2.1.

Proof. [of Lemma 2.1] Pick one $K \in \mathcal{M}$ and, without loss of generality, assume $0 \in K$. Then define the lifting operator, *cf.* the "Koszul lifting" [3, Sect. 3.2],

$$\mathbf{w} \mapsto \mathcal{L}\,\mathbf{w}\ , \quad \mathcal{L}\,\mathbf{w}(\boldsymbol{x}) := \tfrac{1}{3}\mathbf{w}(\boldsymbol{x}) \times \boldsymbol{x}\ , \quad \boldsymbol{x} \in K\ . \tag{2.9}$$

Elementary calculations reveal that for any $\mathbf{w} \equiv \text{const}^3$

$$\mathbf{curl}\,\mathcal{L}\,\mathbf{w} = \mathbf{w}\ , \tag{2.10}$$

$$\left\| \mathcal{L}\,\mathbf{w} \right\|_{L^2(K)} \leq h_K \left\| \mathbf{w} \right\|_{L^2(K)}\ , \tag{2.11}$$

$$\mathcal{L}\,\mathbf{w} \in \mathbf{U}(K)\ . \tag{2.12}$$

The continuity (2.11) permits us to extend $\mathcal{L}$ to $(L^2(K))^3$.

Given $\Psi \in (H^1(K))^3$ with $\mathbf{curl}\,\Psi \equiv \text{const}^3$, by (2.12) we know $\mathcal{L}\,\mathbf{curl}\,\Psi \in (\mathcal{P}_1(K))^3$. Thus, an inverse inequality leads to

$$|\mathcal{L}\,\mathbf{curl}\,\Psi|_{H^1(K)} \leq C h_K^{-1} \|\mathcal{L}\,\mathbf{curl}\,\Psi\|_{L^2(K)} \overset{(2.11)}{\leq} C \|\mathbf{curl}\,\Psi\|_{L^2(K)} \;, \tag{2.13}$$

with $C = C(\rho_K) > 0$. Next, (2.10) implies

$$\mathbf{curl}(\Psi - \mathcal{L}\,\mathbf{curl}\,\Psi) = 0 \quad \Rightarrow \quad \exists p \in H^1(K): \quad \Psi - \mathcal{L}\,\mathbf{curl}\,\Psi = \operatorname{grad} p \;. \tag{2.14}$$

From (2.13) we conclude that $p \in H^2(K)$ and $|p|_{H^2(K)} \leq C|\Psi|_{H^1(K)}$. Moreover, thanks to the commuting diagram property we have

$$\Psi - \Pi_h \Psi = \underbrace{\mathcal{L}\,\mathbf{curl}\,\Psi - \Pi_h\,\mathcal{L}\,\mathbf{curl}\,\Psi}_{=0 \text{ by } (2.12)} + \operatorname{grad}(p - \mathcal{I}_h p) \;, \tag{2.15}$$

which means, by standard estimates for linear interpolation on K,

$$\|\Psi - \Pi_h \Psi\|_{L^2(K)} = |p - \mathcal{I}_h p|_{H^1(K)} \leq C h_K |p|_{H^2(K)} \leq C h_K |\Psi|_{H^1(K)} \;.$$

Summation over all elements finishes the proof. □

As theoretical tools we need "higher order" counterparts of the above finite element spaces. We recall the quadratic Lagrangian finite element space

$$V_2(\mathcal{M}) := \{u_h \in H^1_{\Gamma_D}(\Omega) :\; u_{h|K} \in \mathbb{P}_2(K)\; \forall K \in \mathcal{M}\} \;,$$

and its subspace of quadratic surpluses

$$\widetilde{V}_2(\mathcal{M}) := \{u_h \in V_2(\mathcal{M}) :\; \mathcal{I}_h u_h = 0\} \;.$$

This implies a direct splitting

$$V_2(\mathcal{M}) = V(\mathcal{M}) \oplus \widetilde{V}_2(\mathcal{M}) \;, \tag{2.16}$$

which is unconditionally H^1-stable: there is a $C = C(\rho_{\mathcal{M}}) > 0$ such that

$$C^{-1}|u_h|^2_{H^1(\Omega)} \leq |(Id - \mathcal{I}_h)u_h|^2_{H^1(\Omega)} + |\mathcal{I}_h u_h|^2_{H^1(\Omega)} \leq C|u_h|^2_{H^1(\Omega)} \;, \tag{2.17}$$

for all $u_h \in V_2(\mathcal{M})$.

Next, we examine the space $(V(\mathcal{M}))^3$ of continuous piecewise linear vector fields that vanish on Γ_D. Standard affine equivalence techniques for edge elements, see [25, Sect. 3.6], confirm

$$\exists C = C(\rho_{\mathcal{M}}) > 0 : \quad \|\Pi_h \Psi_h\|_{L^2(\Omega)} \leq C \|\Psi_h\|_{L^2(\Omega)} \quad \forall \Psi_h \in (V(\mathcal{M}))^3 \;. \tag{2.18}$$

Lemma 2.2. *For all $\Psi_h \in (V(\mathcal{M}))^3$ we can find $\widetilde{v}_h \in \widetilde{V}_2(\mathcal{M})$ such that*

$$\Psi_h = \Pi_h \Psi_h + \operatorname{grad} \widetilde{v}_h \;,$$

and, with $C = C(\rho_{\mathcal{M}}) > 0$,

$$C^{-1} \|\Psi_h\|^2_{L^2(\Omega)} \leq \|\Pi_h \Psi_h\|^2_{L^2(\Omega)} + \|\operatorname{grad} \widetilde{v}_h\|^2_{L^2(\Omega)} \leq C \|\Psi_h\|^2_{L^2(\Omega)} \;.$$

For the proof we rely on a very useful insight, which relieves us from all worries concerning the topology of Ω:

LEMMA 2.3. *If* $\mathbf{v} \in \boldsymbol{H}_{\Gamma_D}(\mathbf{curl}\,0, \Omega)$ *and* $\mathbf{\Pi}_h \mathbf{v} = 0$*, then* $\mathbf{v} \in \operatorname{grad} H^1_{\Gamma_D}(\Omega)$.

Proof. Since the mesh covers Ω, the relative homology group $H_1(\Omega; \Gamma_D)$ is generated by a set of edge paths. By definition (2.1) of the d.o.f. of $\mathbf{U}(\mathcal{M})$, the path integrals of $\mathbf{v}$ along all these paths vanish. As an irrotational vector field with vanishing circulation along a complete set of Γ_D-relative fundamental cycles, $\mathbf{v}$ must be a gradient. □

Proof. [of Lemma 2.2] Given $\mathbf{\Psi}_h \in (V(\mathcal{M}))^3$, we decompose it according to

$$\mathbf{\Psi}_h = \mathbf{\Pi}_h \mathbf{\Psi}_h + \underbrace{(Id - \mathbf{\Pi}_h)\mathbf{\Psi}_h}_{=:\operatorname{grad} \widetilde{v}_h} . \tag{2.19}$$

Note that $\mathbf{curl}(Id - \mathbf{\Pi}_h)\mathbf{\Psi}_h$ is piecewise constant with vanishing flux through all triangular faces of $\mathcal{M}$. Then Stokes' theorem teaches that $\mathbf{curl}(Id - \mathbf{\Pi}_h)\mathbf{\Psi}_h = 0$.

By the projector property of $\mathbf{\Pi}_h$, $(Id - \mathbf{\Pi}_h)\mathbf{\Psi}_h$ satisfies the assumptions of Lemma 2.3. Taking into account that, moreover, the field is piecewise linear, it is clear that $(Id - \mathbf{\Pi}_h)\mathbf{\Psi}_h \in \operatorname{grad} V_2(\mathcal{M})$. The stability of the splitting is a consequence of (2.18). □

By definition, the spaces $\mathbf{U}(\mathcal{M})$ and $V(\mathcal{M})$ accommodate the homogeneous boundary conditions on Γ_D. Later, we will also need finite element spaces oblivious of boundary conditions, that is, for the case $\Gamma_D = \emptyset$. These will be tagged by a bar on top, e.g., $\overline{\mathbf{U}}(\mathcal{M})$, $\overline{V}(\mathcal{M})$, etc. The same convention will be employed for notions and operators associated with finite element spaces: if they refer to the particular case $\Gamma_D = \emptyset$, they will be endowed with an overbar, e.g. $\overline{\mathbf{\Pi}}_h$, $\overline{\mathcal{I}}_h$, $\overline{\mathfrak{B}}_{\mathbf{U}}(\mathcal{M})$, $\overline{\mathcal{N}}(\mathcal{M})$, etc.

REMARK 2.4. *The presentation is confined to tetrahedral meshes and lowest order edge elements just for the sake of simplicity. Extension of all results to hexahedral meshes and higher order edge elements is straightforward.*

3. Local mesh refinement. We study the case where the actual finite element mesh $\mathcal{M}_h$ of Ω has been created by successive local refinement of a relatively uniform initial mesh $\mathcal{M}_0$. Concerning $\mathcal{M}_h$ and $\mathcal{M}_0$ the following *asumptions* will be made:

1. Given $\mathcal{M}_0$ and $\mathcal{M}_h$ we can construct a *virtual* refinement hierarchy of $L+1$ *nested* tetrahedral meshes, $L \in \mathbb{N}$:
$$\mathcal{M}_0 \prec \mathcal{M}_1 \prec \mathcal{M}_2 \prec \cdots \prec \mathcal{M}_L = \mathcal{M}_h . \tag{3.1}$$
Please note that the virtual refinement hierarchy may be different from the actual sequence of meshes spawned during adaptive refinement.
2. Inductively, we assign to each tetrahedron $K \in \mathcal{M}_l$ a level $\ell(K) \in \mathbb{N}_0$ by counting the number of subdivisions it took to generate it from an element of $\mathcal{M}_0$.
3. For all $0 \le l < L$ the mesh $\mathcal{M}_{l+1}$ is created by subdividing some or all of the tetrahedra in $\{K \in \mathcal{M}_l : \ell(K) = l\}$.
4. The shape regularity measures of the meshes $\mathcal{M}_l$ are uniformly bounded independently of L.

Refinement may be local, but it must be regular in the following sense, *cf.* [45]: we can find a second sequence of nested tetrahedral meshes of Ω

$$\mathcal{M}_0 = \widehat{\mathcal{M}}_0 \prec \widehat{\mathcal{M}}_1 \prec \widehat{\mathcal{M}}_2 \prec \cdots \prec \widehat{\mathcal{M}}_L . \tag{3.2}$$

that satisfies

1. $\mathcal{M}_l \prec \widehat{\mathcal{M}}_l$ and $\{K \in \mathcal{M}_l : \ell(K) = l\} \subset \widehat{\mathcal{M}}_l$, $l = 0, \ldots, L$,
2. that the shape regularity measure $\rho_{\widehat{\mathcal{M}}_l}$ is bounded independently of l,
3. and that there exist two constants $C > 0$ and $0 < \theta < 1$ independent of l and L such that

$$C^{-1}\theta^l \leq h_K \leq C\theta^l \quad \forall K \in \widehat{\mathcal{M}}_l \ , \quad 0 \leq l \leq L \ . \tag{3.3}$$

   This means that the family $\{\widehat{\mathcal{M}}_l\}_l$ is quasi-uniform. Hence, it makes sense to refer to a mesh width $h_l := \max\{h_K,\ K \in \widehat{\mathcal{M}}_l\}$ of $\widehat{\mathcal{M}}_l$. It decreases geometrically for growing l.

Popular tetrahedral refinement schemes generate meshes that meet the requirements. A first example is local regular refinement with hanging nodes [1], which, in each step, splits a subset of the tetrahedra of the current mesh into eight smaller ones. An illustrative 2D[1] example with hanging nodes is depicted in Figure 3.1. The accompanying sequence $\{\widehat{\mathcal{M}}_l\}_{0 \leq l \leq L}$ is produced by global regular refinement, which implies (3.3) with $\theta = \frac{1}{2}$. Uniform shape-regularity can also be guaranteed for repeated regular refinement of tetrahedra, see [8].

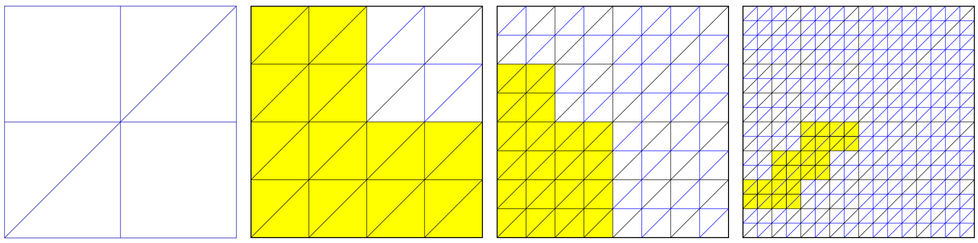

FIG. 3.1. *Virtual refinement hierarchy for 2D triangular meshes. The quasi-uniform sequence* $\{\widehat{\mathcal{M}}_l\}_{0 \leq l \leq L}$ *is sketched in blue. Elements of* $\mathcal{M}_l$ *eligible for further subdivision are marked yellow.*

Another viable refinement scheme is to use bisection of tetrahedra. This procedure refers to splitting a tetrahedron into two by promoting the midpoint of the so-called refinement edge to a new vertex. Variants of bisection differ by the selection of refinement edges: The iterative bisection strategy by Bänsch [5] needs the intermediate handling of hanging nodes. The recursive bisection strategies of [29, 31] do not create such hanging nodes and, therefore, are easier to implement. But for special $\mathcal{M}_0$, the two recursive algorithms result in exactly the same tetrahedral meshes as the iterative algorithm. Since our implementation relies on the bisection algorithm of [29], we outline its bisection policy in the following. For more information on bisection algorithms, we refer to [38].

For the recursive bisection algorithm of [29], the bisections of tetrahedra are totally determined by the local vertex numbering of $\mathcal{M}_0$, plus a prescribed type for every element in $\mathcal{M}_0$. Each tetrahedron K is endowed with the local indices 0, 1, 2, and 3 for its vertices. The refinement edge of each element is always set to be the edge connecting vertex 0 and vertex 1. After bisection of K, the "child tetrahedron" of K which contains vertex 0 of K is denoted by Child[0] and the other one is denoted by

[1] For ease of visualization, we will always elucidate geometric concepts in two-dimensional settings. Their underlying ideas are the same in 2D and 3D.

Child[1]. The types of Child[0] and Child[1] are defined by

$$\mathsf{type}(\text{Child}[0]) = \mathsf{type}(\text{Child}[1]) = (\mathsf{type}(K) + 1) \mod 3.$$

The new vertex at the midpoint of the refinement edge of K is always numbered by 3 in Child[0] and Child[1]. The four vertices of K are numbered in Child[0] and Child[1] as follows (see Fig. 3.2):

$$\begin{aligned}
&\text{In Child}[0]: \quad (0,2,3) \to (0,1,2), \\
&\text{In Child}[1]: \quad (0,2,3) \to (0,2,1) \quad \text{if} \quad \mathsf{type}(K) = 0, \\
&\text{In Child}[1]: \quad (0,2,3) \to (0,1,2) \quad \text{if} \quad \mathsf{type}(K) > 0.
\end{aligned}$$

This recursive bisection creates only a small number of similarity classes of tetrahedra (see [29, 38]).

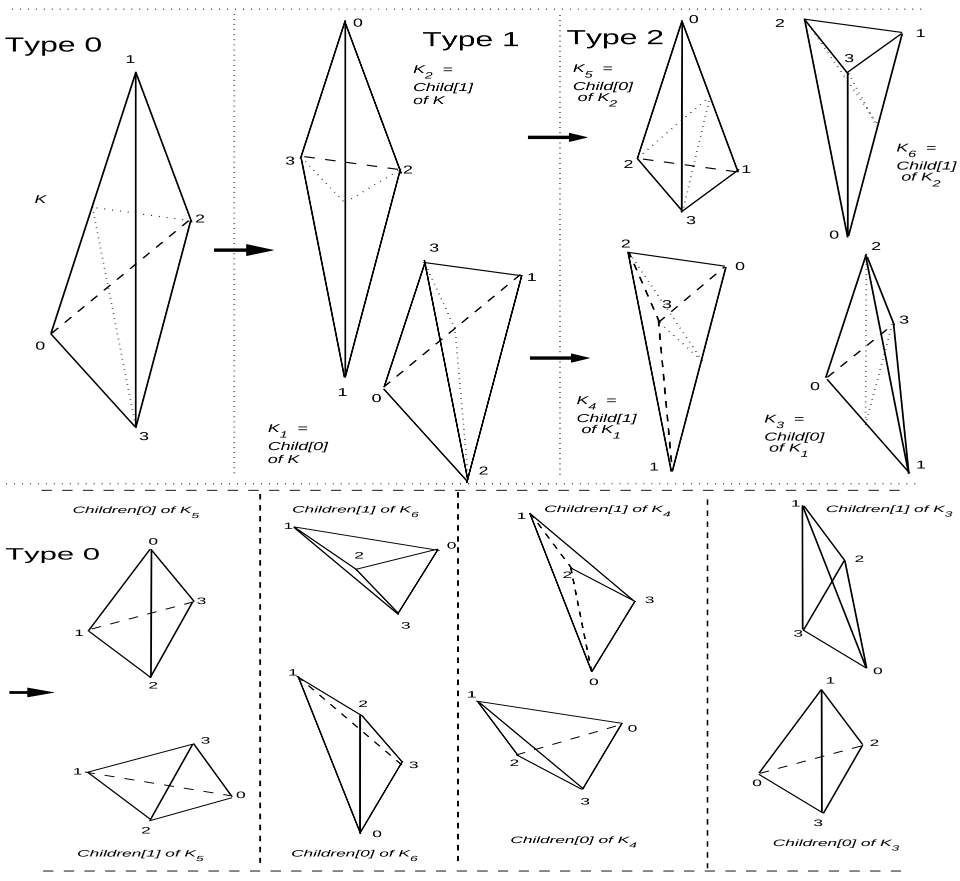

FIG. 3.2. *Bisection of tetrahedra in the course of recursive bisection. Assignment of types to children*

Fig 3.3 shows a 2D example of the recursive bisection refinement (the algorithm for 2D case is called “the newest vertex bisection” in [32]). Similar to the 3D algorithm, for any element K, its three vertices are locally numbered by 0, 1, and 2, its refinement edge is the edge between vertex 0 and 1. The newly created vertex in the two children of K are numbered by 2. In the child element containing vertex 0 of K, vertex 0 and

2 of K are renumbered by 1 and 0 respectively. In the other child element, vertex 1 and 2 of K are renumbered by 0 and 1 respectively.

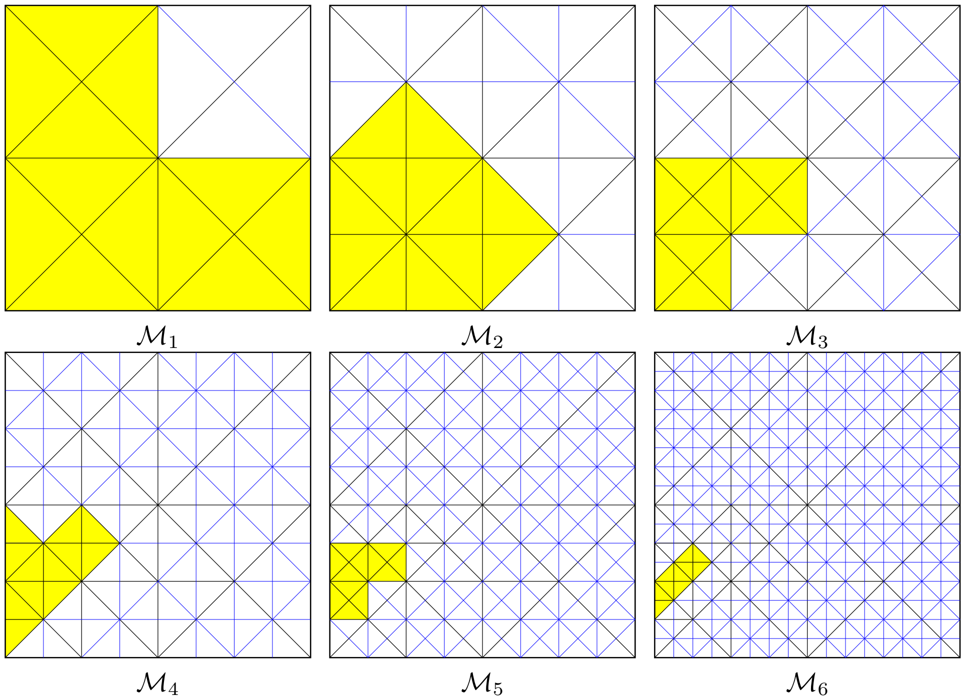

FIG. 3.3. *Virtual refinement hierarchy for 2D triangular meshes emerging in the course of successive local newest vertex bisection refinement of $\mathcal{M}_0$ from Fig. 3.1. Accompanying quasi-uniform meshes outlined in blue, maximally refined triangles marked yellow.*

In order to keep the mesh conforming during refinements, the bisection of an edge is only allowed when such an edge is the refinement edge for all elements which share this edge. If a tetrahedron has to be refined, we have to loop around its refinement edge and collect all elements at this edge to create an refinement patch. Then this patch is refined by bisecting the common refinement edge. For any mesh $\mathcal{M}_l$ an associated "quasi-uniform" mesh $\widehat{\mathcal{M}_l}$ according to (3.2), $\mathcal{M}_l \prec \widehat{\mathcal{M}_l}$, is obtained as follows: the elements in $\{K \in \mathcal{M}_l : \ \ell(K) < l\}$ undergo bisection until $\ell(K) = l$ for any $K \in \widehat{\mathcal{M}_l}$.

We still have to make sure that the recursive bisection allows the definition of a virtual refinement hierarchy. Thus, let $\mathcal{M}_h = \mathcal{M}_L$ be generated from the initial mesh $\mathcal{M}_0$ by the bisection algorithm in [29]. Denote by $\mathcal{M}_{\text{hier}}$ the set of all tetrahedra created during the bisection process, i.e., for any $K \in \mathcal{M}_{\text{hier}}$, there is a $K' \in \mathcal{M}_h$ such that either $K' = K$ or K' is created by refining K. Then, the virtual meshes $\mathcal{M}_l$, $0 < l < L$ can be defined as

$$\mathcal{M}_l := \{K \in \mathcal{M}_{\text{hier}} : \ \ell(K) \leq l\} \quad 0 < l < L\,. \tag{3.4}$$

In the following, we are going to prove that each $\mathcal{M}_l$ is a conforming mesh, that is, no hanging nodes occur in $\mathcal{M}_l$, $0 \leq l \leq L$. The proof depends on some mild assumptions on $\mathcal{M}_0$ (see assumptions (A1) and (A2) in [29]) which will be taken for granted.

LEMMA 3.1. *[29, Lemmas 2,3] Let $T, T' \in \mathcal{M}_h$ be a pair of tetrahedra sharing a face $F = K \cap K'$. It holds true that*

1. *if T contains the refinement edge of T' and vice versa, then they have the same refinement edge,*
2. *if F contains the refinement edges of both K and K', then $\ell(K) = \ell(K')$,*
3. *if F contains the refinement edge of K, but does not contain the refinement edge of K', then $\ell(K) = \ell(K') + 1$,*
4. *if F does not contain the refinement edges of K and K', then $\ell(K) = \ell(K')$.*

LEMMA 3.2. *The meshes $\mathcal{M}_l$, $0 \le l \le L$, according to* (3.4) *are conforming meshes.*

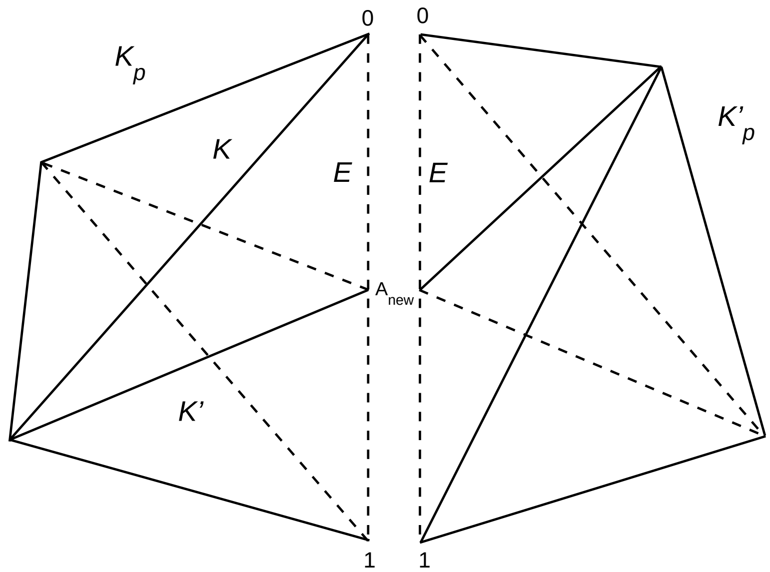

FIG. 3.4. *The patch around a refinement edge E with vertex 0 and 1. $\ell(K) = \ell(K') = L$ and $\ell(K_p) = \ell(K'_p) = L - 1$.*

Proof. We are going to prove the lemma by backward induction starting from $l = L$. Since $\mathcal{M}_L = \mathcal{M}_h$ is conforming, for any $K \in \mathcal{M}_L$ satisfying $\ell(K) = L$, there exists a brother of K, denoted by $K' \in \mathcal{M}_L$, such that $\ell(K') = L$ and $K_p := K \cup K' \in \mathcal{M}_{L-1}$. Here K_p is called the parent of K and K' with $\ell(K_p) = L - 1$ (see Fig. 3.4).

Let E be the refinement edge of K_p. By the recursive bisection algorithm, E must be the common refinement edge of all tetrahedra in the refinement patch:

$$P_E = \bigcup \{ \overline{K'_p} : \ K'_p \in \mathcal{M}_{L-1} \text{ and } E \subset \overline{K'_p} \}.$$

By Lemma 3.1, $\ell(K'_p) = L - 1$ for any $K'_p \subset P_E$ and the midpoint of E, denoted by A_{new}, is the unique new vertex of $\mathcal{M}_L$ in P_E. We conclude that

$$P_E = \bigcup \{ \overline{K} : \ K \in \mathcal{M}_L, \ \ell(K) = L, \text{ and } A_{\text{new}} \text{ is a vertex of } K \}.$$

Coarsen the sub-mesh $\mathcal{M}_{L|P_E}$ by removing the vertex A_{new} and all edges related to it and adding E to this patch. Thus a conforming sub-mesh $\mathcal{M}_{L-1|P_E}$ is obtained. Do above coarsening process for every element $K \in \mathcal{M}_L$ with $\ell(K) = L$. This proves that $\mathcal{M}_{L-1}$ is conforming.

Finally, an induction argument confirms that $\mathcal{M}_l$ is conforming, $l = L-2, \cdots, 1$. ∎

4. Local multigrid. To begin with, we introduce nested refinement zones as open subsets of Ω:

$$\omega_l := \text{interior}\Big(\bigcup\{\overline{K} : \, K \in \mathcal{M}_h, \, \ell(K) \geq l\}\Big) \subset \Omega \,, \tag{4.1}$$

see Fig. 4.1 and Fig. 4.2. The notion of refinement zones allows a concise definition of the local multilevel decompositions of the finite element spaces $V(\mathcal{M}_h)$ and $\mathbf{U}(\mathcal{M}_h)$ that underly the local multigrid method.

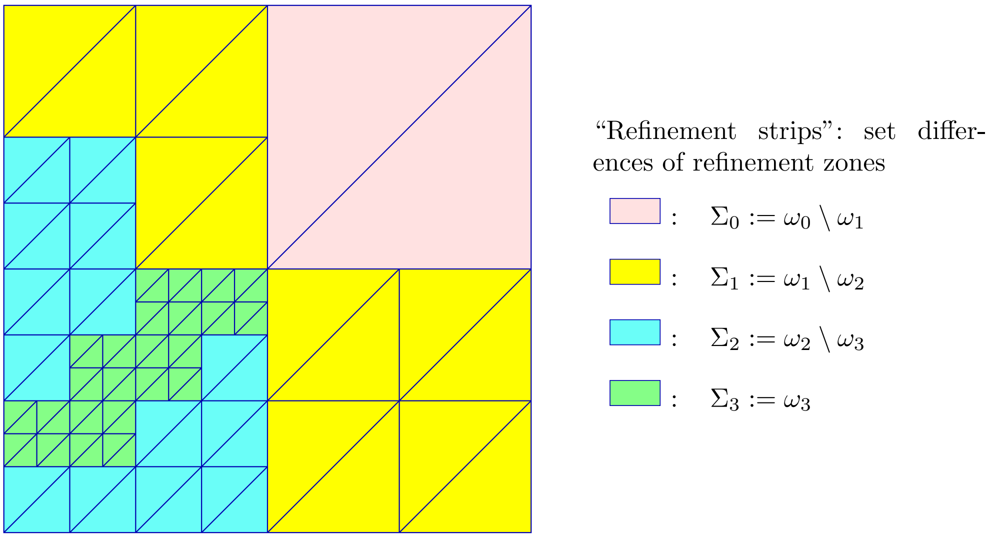

FIG. 4.1. *Refinement zones for the 2D refinement hierarchy of Figure 3.1.*

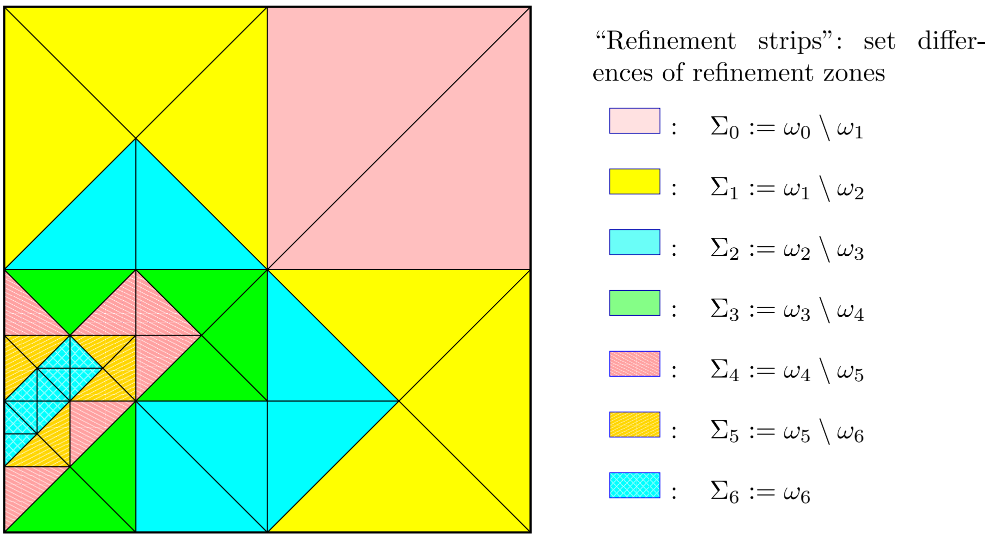

FIG. 4.2. *Refinement zones for the 2D refinement hierarchy of Figure 3.3.*

We introduce local multigrid from the perspective of multilevel successive subspace correction (SSC) [46–48]. First, we give an abstract description for a linear variational problem

$$u \in H: \quad \mathsf{a}(u,v) = f(v) \quad \forall v \in H \;, \tag{4.2}$$

involving a positive definite bilinear form a on a Hilbert space H. The method is completely defined after we have provided a finite subspace decomposition

$$H = \sum_{j=0}^{J} H_j \;, \quad H_j \subset H \text{ closed subspaces, } j = 0,\dots,J,\; J \in \mathbb{N} \;. \tag{4.3}$$

Then the correction scheme implementation of one step of SSC acting on the iterate u^{m-1} reads:

for $m = 1, 2, \cdots$
  $u_0^{m-1} = u^{m-1}$
  for $j = 0, 1, \cdots, J$
    Let $e_j \in H_j$ solve

$$\mathsf{a}(e_j, v_j) = f(v_j) - \mathsf{a}(u_{j-1}^{m-1}, v_j) \quad \forall\, v_j \in H_j$$

    $u_j^{m-1} = u_{j-1}^{m-1} + e_j$
  endfor
  $u^m = u_J^{m-1}$
endfor

This amounts to a stationary linear iterative method with error propagation operator

$$E = (I - P_J)(I - P_{J-1}) \cdots (I - P_0) \;, \tag{4.4}$$

where $P_j : H \mapsto H_j$ stands for the Galerkin projection defined through

$$\mathsf{a}(P_j v, v_j) = \mathsf{a}(v, v_j) \quad \forall\, v_j \in H_j. \tag{4.5}$$

The convergence theory of SSC for an inner product a rests on two assumptions. The first one concerns the *stability of the space decomposition*. We assume that there exists a constant C_{stab} independent of J such that

$$\inf \Big\{ \sum_{j=0}^{J} \|v_j\|_A^2 : \; \sum_{j=0}^{J} v_j = v \Big\} \le C_{\text{stab}} \|v\|_A^2 \quad \forall\, v \in H. \tag{4.6}$$

The second assumption is a *strengthened Cauchy-Schwartz inequality*, namely, there exist two constants $0 \le q < 1$ and C_{orth} independent of j and k such that

$$\mathsf{a}(v_j, v_k) \le C_{\text{orth}} q^{|k-j|} \|v_j\|_A \|v_k\|_A \quad \forall\, v_j \in H_j,\; v_k \in H_k \;. \tag{4.7}$$

The above inequality states a kind of quasi-orthogonality between the subspaces. From [46, Theorem 4.4] and [50, Theorem 5.1] we cite the following central convergence theorem:

THEOREM 4.1. *Provided that* (4.6) *and* (4.7) *hold, the convergence rate of Algorithm SSC is bounded by*

$$\|E\|_A^2 \le 1 - \frac{1}{C_{\text{stab}}(1+\Theta)^2} \quad \textit{with} \quad \Theta = C_{\text{orth}} \frac{1+q}{1-q}, \tag{4.8}$$

where the operator norm is defined by

$$\|E\|_A := \sup_{v \in H, v \neq 0} \frac{\|Ev\|_A}{\|v\|_A}.$$

The bottom line is that the subspace splitting (4.3) already provides a full description of the method. Showing that both constants C_{stab} from (4.6) and C_{orth} from (4.7) can be chosen independently of the number L of refinement levels is the challenge in asymptotic multigrid analysis.

In concrete terms, the role of the linear variational problem (4.2) is played by (1.1) considered on the edge element space $\mathbf{U}(\mathcal{M}_h)$, which replaces the Hilbert space H. To define the local multilevel decomposition of $\mathbf{U}(\mathcal{M}_h)$, we define "sets of new basis functions" on the various refinement levels

$$\begin{aligned} &\mathfrak{B}_V^0 := \mathfrak{B}_V(\mathcal{M}_0), \quad \mathfrak{B}_V^l := \{b_h \in \mathfrak{B}_V(\mathcal{M}_l) : \operatorname{supp} b_h \subset \overline{\omega}_l\}, \\ &\mathfrak{B}_{\mathbf{U}}^0 := \mathfrak{B}_{\mathbf{U}}(\mathcal{M}_0), \quad \mathfrak{B}_{\mathbf{U}}^l := \{\mathbf{b}_h \in \mathfrak{B}_{\mathbf{U}}(\mathcal{M}_l) : \operatorname{supp} \mathbf{b}_h \subset \overline{\omega}_l\}, \end{aligned} \quad 1 \leq l \leq L. \tag{4.9}$$

A 2D drawing of the sets $\mathfrak{B}_V^l$ is given in Fig. 4.3 where $\Gamma_D = \partial\Omega$. Note that we also have to deal with $V(\mathcal{M}_h)$, because, as suggested by the reasoning in [24], a local multilevel decomposition of $\mathbf{U}(\mathcal{M}_h)$ has to incorporate an appropriate local multilevel decomposition of $V(\mathcal{M}_h)$.

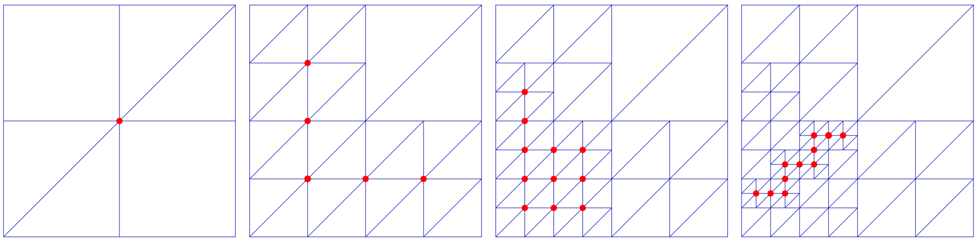

$l = 0$ $l = 1$ $l = 2$ $l = 3$

FIG. 4.3. *Active vertices (red) carrying "tent functions" in $\mathfrak{B}_V^l$, $\Gamma_D = \partial\Omega$, refinement hierarchy of Fig. 3.1*

Then, a possible local multigrid iteration for the linear system of equations arising from a finite element Galerkin discretization of a $H^1_{\Gamma_D}(\Omega)$-elliptic variational problem boils down to a successive subspace correction method based on the local multilevel decomposition

$$V(\mathcal{M}_h) = V(\mathcal{M}_0) + \sum_{l=1}^{L} \sum_{b_h \in \mathfrak{B}_V^l} \operatorname{Span}\{b_h\}. \tag{4.10}$$

Similarly, the local multilevel splitting of $\mathbf{U}(\mathcal{M}_h)$ is based on the multilevel decomposition

$$\mathbf{U}(\mathcal{M}_h) = \mathbf{U}(\mathcal{M}_0) + \sum_{l=1}^{L} \sum_{b_h \in \mathfrak{B}_V^l} \operatorname{Span}\{\operatorname{grad} b_h\} + \sum_{l=1}^{L} \sum_{\mathbf{b}_h \in \mathfrak{B}_{\mathbf{U}}^l} \operatorname{Span}\{\mathbf{b}_h\}. \tag{4.11}$$

These choices are motivated both by the design of multigrid methods for (1.1) and $\mathbf{U}(\mathcal{M})$ in the case of uniform refinement and local multigrid approaches to $H^1_{\Gamma_D}(\Omega)$-elliptic variational problems after discretization by means of linear finite elements [32, 45]. The occurrence of gradients of “tent functions” b_h in (4.11) is related to the *hybrid local relaxation*, which is essential for the performance of multigrid in $\boldsymbol{H}(\mathbf{curl},\Omega)$, see [24] for a rationale. A rigorous justification will emerge during the theoretical analysis in the following sections. It will establish the following main theorem.

THEOREM 4.2 (Asymptotic convergence of local multigrid for edge elements). *Under the assumptions on the meshes made above and allowing at most one hanging node per edge, the decomposition* (4.11) *leads to an SSC iteration whose convergence rate is bounded away from* 1 *uniformly in the number* L *of refinement steps.*

5. Stability. First we tackle the stability estimate (4.6) for the local multilevel decomposition (4.10), which is implicitly contained in (4.11).

5.1. Local quasi-interpolation onto $V(\mathcal{M})$. Quasi-interpolation operators are projectors onto finite element spaces that have been devised to accommodate two conflicting goals: locality and boundedness in weak norms [17,35,39,40]. We resort to a construction employing local linear L^2-dual basis functions.

For a generic tetrahedron K define ψ_j^K, $j = 1,2,3,4$, by $L^2(K)$-duality to the barycentric coordinate functions λ_i, $i = 1,2,3,4$, of K:

$$\psi_j^K \in \mathbb{P}_1(K): \quad \int_K \psi_j^K(\boldsymbol{x})\lambda_i(\boldsymbol{x})\,\mathrm{d}\boldsymbol{x} = \delta_{ij}\ , \quad i,j\in\{1,\dots,4\}\ . \tag{5.1}$$

Computing an explicit representation of the ψ_j^K we find

$$C^{-1} \le |K|\,\left\|\psi_j^K\right\|^2_{L^2(K)} \le C \quad , \quad C^{-1} \le \left\|\psi_j^K\right\|_{L^1(K)} \le C\ , \tag{5.2}$$

with an absolute constant $C > 0$. We can regard ψ_j^K as belonging to the j-th vertex of K. Thus, we will also write $\psi_{\boldsymbol{p}}^K$, $\boldsymbol{p}\in\mathcal{N}(K)$, $\mathcal{N}(K)$ the set of vetices of K.

We assume a generic tetrahedral mesh $\mathcal{M}$ of Ω. In order to introduce quasi-interpolation operators we take for granted some “node→cell”–assignment, a mapping $\overline{\mathcal{N}}(\mathcal{M}) \mapsto \mathcal{M}$, $\boldsymbol{p}\in\overline{\mathcal{N}}(\mathcal{M}) \mapsto K_{\boldsymbol{p}} \in \mathcal{M}$.

DEFINITION 5.1. *Writing* $\{b_{\boldsymbol{p}}\}_{\boldsymbol{p}\in\mathcal{N}(\mathcal{M})} := \mathfrak{B}_V(\mathcal{M})$, *define the local quasi-interpolation operator*

$$\mathsf{Q}_h : \begin{cases} L^2(\Omega) & \mapsto \quad V(\mathcal{M}) \\ \quad u & \mapsto \quad \sum_{\boldsymbol{p}\in\mathcal{N}(\mathcal{M})} \int_{K_{\boldsymbol{p}}} \psi_{\boldsymbol{p}}^{K_{\boldsymbol{p}}}(\boldsymbol{x})u(\boldsymbol{x})\,d\boldsymbol{x}\cdot b_{\boldsymbol{p}}\ . \end{cases} \tag{5.3}$$

Analoguously, we introduce the local quasi-interpolation $\overline{\mathsf{Q}}_h : L^2(\Omega) \mapsto \overline{V}(\mathcal{M})$.

We point out that Q_h respects $u = 0$ on Γ_D, because the sum does not cover basis functions attached to vertices on Γ_D. From (5.1) it is also evident that both Q_h and $\overline{\mathsf{Q}}_h$ are projections, for instance,

$$\mathsf{Q}_h u_h = u_h \quad \forall\, u_h \in V(\mathcal{M})\ . \tag{5.4}$$

Moreover, they satisfy the following strong continuity and approximation properties:

LEMMA 5.2. *The quasi-interpolation operators from Def. 5.1 allow the estimates (set* $\Gamma_D = \emptyset$ *for* $\overline{\mathsf{Q}}_{\mathcal{M}}$*)*

$$\exists C = C(\rho_{\mathcal{M}}): \qquad \left\|\mathsf{Q}_h u\right\|_{L^2(\Omega)} \le C\left\|u\right\|_{L^2(\Omega)} \quad \forall\, u\in L^2(\Omega)\ , \tag{5.5}$$

$$\exists C = C(\rho_{\mathcal{M}},\Omega,\Gamma_D): \qquad \left|\mathsf{Q}_h u\right|_{H^1(\Omega)} \le C|u|_{H^1(\Omega)} \quad \forall\, u\in H^1_{\Gamma_D}(\Omega)\ , \tag{5.6}$$

$$\exists C = C(\rho_{\mathcal{M}},k): \ \left\|h^{-k}(u-\mathsf{Q}u)\right\|_{L^2(\Omega)} \le C|u|_{H^k(\Omega)} \quad \forall\, u\in H^k(\Omega)\cap H^1_{\Gamma_D}(\Omega)\ , \tag{5.7}$$

and $k = 1, 2$.

Proof. [Part I] Continuity in $L^2(\Omega)$ is a simple consequence of the stability (2.6) of the nodal bases $\mathfrak{B}_V(\mathcal{M})$ and of the Cauchy-Schwarz inequality:

$$\begin{aligned}
\|\mathsf{Q}_h u\|^2_{L^2(\Omega)} &\leq C \sum_{\boldsymbol{p}\in\mathcal{N}(\mathcal{M})} |\mathsf{Q}_h u(\boldsymbol{p})|^2 \, \|b_{\boldsymbol{p}}\|^2_{L^2(\Omega)} \\
&= C \sum_{\boldsymbol{p}\in\mathcal{N}(\mathcal{M})} \left| \int_{K_{\boldsymbol{p}}} \psi_{\boldsymbol{p}}^{K_{\boldsymbol{p}}}(\boldsymbol{x}) u(\boldsymbol{x}) \, d\boldsymbol{x} \right|^2 \|b_{\boldsymbol{p}}\|^2_{L^2(\Omega)} \\
&\leq C \sum_{\boldsymbol{p}\in\mathcal{N}(\mathcal{M})} \left\| \psi_{\boldsymbol{p}}^{K_{\boldsymbol{p}}} \right\|^2_{L^2(K_{\boldsymbol{p}})} \|b_{\boldsymbol{p}}\|^2_{L^2(\Omega)} \, \|u\|^2_{L^2(K_{\boldsymbol{p}})} \leq C \, \|u\|^2_{L^2(\Omega)} \ ,
\end{aligned}$$

with $C = C(\rho_{\mathcal{M}}) > 0$, because $\left\| \psi_{\boldsymbol{p}}^{K_{\boldsymbol{p}}} \right\|^2_{L^2(K_{\boldsymbol{p}})} \|b_{\boldsymbol{p}}\|^2_{L^2(\Omega)} \leq C$, too. ☐

The following estimate is instrumental in establishing continuity of Q_h in $H^1_{\Gamma_D}(\Omega)$:

THEOREM 5.3 (Generalized Hardy inquality).

$$\exists C = C(\Omega, \Gamma_D) > 0 : \quad \int\limits_{\Omega} \left| \frac{u}{\operatorname{dist}(\boldsymbol{x}, \Gamma_D)} \right|^2 \mathrm{d}\boldsymbol{x} \leq C |u|^2_{H^1(\Omega)} \quad \forall u \in H^1_{\Gamma_D}(\Omega) \ .$$

Proof. By density it suffices to consider $u \in C^\infty(\overline{\Omega})$, $\operatorname{supp}(u) \cap \Gamma_D = \emptyset$. Using a partition of unity, we can confine the estimate to neighborhoods of Γ_D, in which $\partial\Omega$ is the graph of a Lipschitz-continuous function. Thus, after bi-Lipschitz transformations, we need only investigate three canonical situations, see Fig. 5.1:

1. $\Gamma_D = \{z = 0\}$, for which the 1D Hardy inequality gives the estimate, see the proof of Thm. 1.4.4.4 in [22].
2. $\Gamma_D = \{z = 0 \ \wedge \ x > 0\}$, which can be treated using polar coordinates in the (x, z)-plane and then integrating in y-direction:

$$\int\limits_0^\infty \int\limits_0^\pi \left| \frac{u(r,\varphi)}{r} \right|^2 \mathrm{d}\varphi \, r \, \mathrm{d}r \leq \int\limits_0^\infty \int\limits_0^\pi \left| \frac{\pi}{r} \frac{\partial u}{\partial \varphi}(r,\varphi) \right|^2 \mathrm{d}\varphi \, r \, \mathrm{d}r \leq \pi^2 \int\limits_{z>0} |\operatorname{grad}_{x,z} u|^2 \, \mathrm{d}x \mathrm{d}z \ .$$

3. $\Gamma_D = \{z = 0 \wedge x > 0 \wedge y > 0\}$, for which we obtain a similar estimate using spherical coordinates.

This ends the proof. ☐

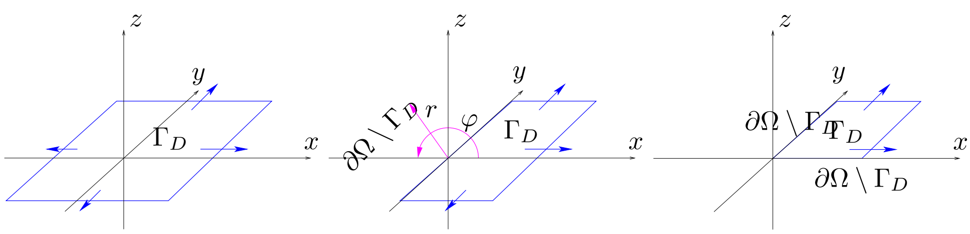

$\Gamma_D = \{z = 0\}$ $\Gamma_D = \{z = 0 \ \wedge \ x > 0\}$ $\Gamma_D = \{z = 0 \wedge x > 0 \wedge y > 0\}$

FIG. 5.1. *Canonical situations to be examined in the proof of Thm. 5.3*

Proof. [of Lemma 5.2, part II] In order to tackle the $H^1(\Omega)$-continuity of Q_h, we use that $\operatorname{grad} V(\mathcal{M}) \subset \mathbf{U}(\mathcal{M})$ along with the stability estimate (2.4)

$$\|\operatorname{grad} \mathsf{Q}_h u\|^2_{L^2(\Omega)} \leq C \sum_{E=[\boldsymbol{p},\boldsymbol{q}]\in\mathcal{E}(\mathcal{M})} (\mathsf{Q}_h u(\boldsymbol{p}) - \mathsf{Q}_h u(\boldsymbol{q}))^2 \, \|\mathbf{b}_E\|^2_{L^2(\Omega)} \ , \tag{5.8}$$

with the notation $\{\mathbf{b}_E\}_{E\in\mathcal{E}(\mathcal{M})} := \mathfrak{B}_{\mathbf{U}}(\mathcal{M})$.

(i) for the case $E = [\boldsymbol{p},\boldsymbol{q}] \in \mathcal{E}(\mathcal{M})$, $\boldsymbol{p},\boldsymbol{q} \notin \Gamma_D$, we adapt arguments from [39]. For any $u \in H^1_{\Gamma_D}(\Omega)$, by (5.1), we have the identity

$$|(\mathsf{Q}_h u)(\boldsymbol{p}) - (\mathsf{Q}_h u)(\boldsymbol{q})| = \Big| \int\limits_{K_{\boldsymbol{p}}} \int\limits_{K_{\boldsymbol{q}}} \psi_{\boldsymbol{p}}^{K_{\boldsymbol{p}}}(\boldsymbol{x}) \psi_{\boldsymbol{q}}^{K_{\boldsymbol{q}}}(\boldsymbol{y}) (u(\boldsymbol{x}) - u(\boldsymbol{y})) \, \mathrm{d}\boldsymbol{y} \mathrm{d}\boldsymbol{x} \Big|$$

$$= \Big| \int\limits_{K_{\boldsymbol{p}}} \int\limits_{K_{\boldsymbol{q}}} \psi_{\boldsymbol{p}}^{K_{\boldsymbol{p}}}(\boldsymbol{x}) \psi_{\boldsymbol{q}}^{K_{\boldsymbol{q}}}(\boldsymbol{y}) \int\limits_0^1 \operatorname{grad} u(\boldsymbol{y} + \tau(\boldsymbol{x}-\boldsymbol{y})) \cdot (\boldsymbol{x}-\boldsymbol{y}) \, \mathrm{d}\tau \, \mathrm{d}\boldsymbol{y} \mathrm{d}\boldsymbol{x} \Big| \ .$$

Then split the innermost integral and transform

$$\int_0^1 f(\boldsymbol{y} + \tau(\boldsymbol{x}-\boldsymbol{y})) \, \mathrm{d}\tau = \int_{\frac{1}{2}}^1 f(\boldsymbol{y} + \tau(\boldsymbol{x}-\boldsymbol{y})) \, \mathrm{d}\tau + \int_{\frac{1}{2}}^1 f(\boldsymbol{x} + \tau(\boldsymbol{y}-\boldsymbol{x})) \, \mathrm{d}\tau \ .$$

We infer

$$\begin{aligned} &|(\mathsf{Q}_h u)(\boldsymbol{p}) - (\mathsf{Q}_h u)(\boldsymbol{q})| \\ &\qquad \leq \int\limits_{\frac{1}{2}}^1 \int\limits_{K_{\boldsymbol{p}}} \int\limits_{K_{\boldsymbol{q}}} |\psi_{\boldsymbol{p}}^{K_{\boldsymbol{p}}}(\boldsymbol{x})| |\psi_{\boldsymbol{q}}^{K_{\boldsymbol{q}}}(\boldsymbol{y})| \, |\operatorname{grad} u(\boldsymbol{y} + \tau(\boldsymbol{x}-\boldsymbol{y}))| |\boldsymbol{x}-\boldsymbol{y}| \, \mathrm{d}\boldsymbol{y} \mathrm{d}\boldsymbol{x} \mathrm{d}\tau \\ &\qquad\quad + \int\limits_{\frac{1}{2}}^1 \int\limits_{K_{\boldsymbol{p}}} \int\limits_{K_{\boldsymbol{q}}} |\psi_{\boldsymbol{p}}^{K_{\boldsymbol{p}}}(\boldsymbol{x})| |\psi_{\boldsymbol{q}}^{K_{\boldsymbol{q}}}(\boldsymbol{y})| \, |\operatorname{grad} u(\boldsymbol{x} + \tau(\boldsymbol{y}-\boldsymbol{x}))| \, |\boldsymbol{x}-\boldsymbol{y}| \, \mathrm{d}\boldsymbol{y} \mathrm{d}\boldsymbol{x} \mathrm{d}\tau \end{aligned}$$

The transformation formula for integrals reveals

$$\int_K f(\boldsymbol{x} + \tau(\boldsymbol{y}-\boldsymbol{x})) \, \mathrm{d}\boldsymbol{y} = \tau^{-3} \int_{K'} f(\boldsymbol{z}) \, \mathrm{d}\boldsymbol{z} \ , \quad K' := \boldsymbol{x} + \tau(K - \boldsymbol{x}) \ .$$

Appealing to the bounds for $\left\|\psi_j^K\right\|_{L^2(K)}$, $\left\|\psi_j^K\right\|_{L^1(K)}$, $K \in \mathcal{M}$, from (5.2), the Cauchy-Schwarz inequality yields

$$\begin{aligned} &|(\mathsf{Q}_h u)(\boldsymbol{p}) - (\mathsf{Q}_h u)(\boldsymbol{q})| \, \|\mathbf{b}_E\|_{L^2(\Omega)} \\ &\qquad \leq C \underbrace{\left[\frac{|\boldsymbol{p}-\boldsymbol{q}| \, \|\mathbf{b}_E\|_{L^2(\Omega)}}{\min\{|K_{\boldsymbol{q}}|^{\frac{1}{2}}, |K_{\boldsymbol{p}}|^{\frac{1}{2}}\}} \right]}_{\leq C = C(\rho_{\mathcal{M}})} \int_{\frac{1}{2}}^1 \tau^{-3/2} \, \mathrm{d}\tau \cdot |u|_{H^1(\langle\Omega_E\rangle)} \ . \end{aligned} \tag{5.9}$$

Here $\langle\Omega_E\rangle$ stands for the convex hull of all tetrahedra adjacent to the edge E.

(ii) now consider $E = [\boldsymbol{p}, \boldsymbol{q}] \in \mathcal{E}(\mathcal{M})$, $\boldsymbol{p} \in \Gamma_D$. Then, for any $u \in H^1_{\Gamma_D}(\Omega)$

$$
\begin{aligned}
|(\mathsf{Q}_h u)(\boldsymbol{q}) - (\mathsf{Q}_h u)(\boldsymbol{p})|^2 &= |(\mathsf{Q}_h u)(\boldsymbol{q})|^2 = \left| \int_{K_{\boldsymbol{q}}} \psi_{\boldsymbol{q}}^{K_{\boldsymbol{q}}}(\boldsymbol{x}) u(\boldsymbol{x}) \,\mathrm{d}\boldsymbol{x} \right|^2 \\
= &\left| \int_{K_{\boldsymbol{q}}} \underbrace{\operatorname{dist}(\boldsymbol{x}, \Gamma_D)}_{\leq C|\boldsymbol{p}-\boldsymbol{q}|} \psi_{\boldsymbol{q}}^{K_{\boldsymbol{q}}}(\boldsymbol{x}) \frac{u(\boldsymbol{x})}{\operatorname{dist}(\boldsymbol{x}, \Gamma_D)} \,\mathrm{d}\boldsymbol{x} \right|^2 \leq \frac{C|\boldsymbol{p}-\boldsymbol{q}|^2}{|K_{\boldsymbol{q}}|} \cdot \int\limits_{K_{\boldsymbol{q}}} \left| \frac{u(\boldsymbol{x})}{\operatorname{dist}(\boldsymbol{x}, \Gamma_D)} \right|^2 \mathrm{d}\boldsymbol{x} \\
\leq &\frac{C}{|\boldsymbol{p}-\boldsymbol{q}|} \int\limits_{\Omega_E} \left| \frac{u(\boldsymbol{x})}{\operatorname{dist}(\boldsymbol{x}, \Gamma_D)} \right|^2 \mathrm{d}\boldsymbol{x} \;,
\end{aligned}
$$

with (different) constants $C = C(\rho_{\mathcal{M}}) > 0$.

Combining (5.8), (5.9), using the finite overlap property of $\mathcal{M}$ in the form

$$
\exists C = C(\rho_{\mathcal{M}}) : \quad \sharp\{E \in \mathcal{E}(\mathcal{M}) : \boldsymbol{x} \in \langle \Omega_E \rangle\} \leq C \quad \forall \boldsymbol{x} \in \Omega \;,
$$

and appealing to Thm. 5.3 confirm $|\mathsf{Q}_h u|_{H^1(\Omega)} \leq C|u|_{H^1(\Omega)}$. Observe that the Hardy inequality makes the constant depend on Ω and Γ_D in addition.

The quasi-interpolation error estimate (5.7) results from scaling arguments. Pick $K \in \mathcal{M}$, $u \in H^2(\Omega) \cap H^1_{\Gamma_D}(\Omega)$, and write $\mathcal{I}_K u \in \mathbb{P}_1(K)$ for the linear interpolant of u on K. Thanks to the projection property, we deduce as in Part I of the proof that, with $C = C(\rho_{\mathcal{M}})$,

$$
\begin{aligned}
\|(Id - \mathsf{Q}_h)u\|_{L^2(K)} &= \|(Id - \mathsf{Q}_h)(u - \mathcal{I}_K u)\|_{L^2(K)} \leq C \, \|u - \mathcal{I}_K u\|_{L^2(\Omega_K)} \\
&\leq C h_K^2 |u|_{H^2(\Omega_K)} \;.
\end{aligned}
$$

Here, we wrote $\Omega_K := \bigcup\{\overline{K'} : \overline{K'} \cap K \neq \emptyset\}$, and the final estimate can be shown by a simple scaling argument, *cf.* (2.7). Estimate (5.7) for $k = 1$ follows by scaling arguments and interpolation between the Sobolev spaces $H^2(\Omega_K)$ and $L^2(\Omega_K)$. ☐

5.2. Multilevel splitting of $V(\widehat{\mathcal{M}}_L)$. In this section we revisit the well-known uniform stability of multilevel splittings of $H^1(\Omega)$-conforming Lagrangian finite element functions in the case of mesh hierarchies generated by uniform, *i.e.* non-local, regular refinement.

We take for granted a virtual refinement hierarchy (3.1) of tetrahedral meshes as introduced in Sect. 3 and its accompanying quasi-uniform family of meshes (3.2).

Owing to the inf in (4.6), it is enough to find a concrete family of admissible "candidate" decompositions that enjoys the desired L-uniform stability. We aim for candidates that fit the locally refined mesh hierarchy.

The principal idea is to use a sequence of quasi-interpolation operators $\mathsf{Q}_l : L^2(\Omega) \mapsto V(\widehat{\mathcal{M}}_l)$ based on a judiciously chosen node→element–assignments. For $\widehat{\mathcal{M}}_l$ we introduce a "coarsest neighbor node→element–assignment": First, for any $\boldsymbol{p} \in \mathcal{N}(\widehat{\mathcal{M}}_l)$, $l = 1, \ldots, L$, we pick $K \in \mathcal{M}_l$ such that

$$
\ell(K) = \min\{\ell(K) : \boldsymbol{p} \in \overline{K},\ K \in \mathcal{M}_l\} \;.
$$

Secondly, we select a "coarsest neighbor" $K_{\boldsymbol{p}} \in \widehat{\mathcal{M}}_l$ among those elements of $\widehat{\mathcal{M}}_l$ that are contained in K. This defines a mapping $\mathcal{N}(\widehat{\mathcal{M}}_l) \mapsto \widehat{\mathcal{M}}_l$, $\boldsymbol{p} \mapsto K_{\boldsymbol{p}}$. We write $\overline{\mathsf{Q}}_l : L^2(\Omega) \mapsto \overline{V}(\widehat{\mathcal{M}}_l)$ for the induced quasi-interpolation operator according to Def. 5.1.

Next, we examine the candidate multilevel splitting

$$u_h = \overline{\mathsf{Q}}_0 u_h + \sum_{l=1}^{L} (\overline{\mathsf{Q}}_l - \overline{\mathsf{Q}}_{l-1}) u_h \ , \quad u_h \in V(\widehat{\mathcal{M}}_L) \ . \tag{5.10}$$

LEMMA 5.4. *There holds, with a constant $C > 0$ solely depending on Ω and the uniform bound for the shape regularity measures $\rho_{\widehat{\mathcal{M}}_l}$, $0 \leq l \leq L$,*

$$\left|\overline{\mathsf{Q}}_0 u_h\right|^2_{H^1(\Omega)} + \sum_{l=1}^{L} h_l^{-2} \left\|(\overline{\mathsf{Q}}_l - \overline{\mathsf{Q}}_{l-1}) u_h\right\|^2_{L^2(\Omega)} \leq C |u_h|^2_{H^1(\Omega)} \quad \forall u_h \in V(\widehat{\mathcal{M}}_L) \ . \tag{5.11}$$

Proof. We take the cue from the elegant approach of Bornemann and Yserentant in [9], who discovered how to bring techniques of real interpolation theory of Sobolev spaces [30] to bear on (5.10). The main tools are the so-called K-functionals given by

$$K(t,u)^2 := \inf_{w \in H^2(\Omega)} \left\{ \|u - w\|^2_{L^2(\Omega)} + t^2 \, |w|^2_{H^2(\Omega)} \right\} \ ,$$
$$K_{\mathbb{R}^3}(t,u)^2 := \inf_{w \in H^2(\mathbb{R}^3)} \left\{ \|u - w\|^2_{L^2(\mathbb{R}^3)} + t^2 \, |w|^2_{H^2(\mathbb{R}^3)} \right\} \ .$$

The estimates (5.6) and (5.7) of Lemma 5.2 create a link between the terms in (5.11) and $K(t,u)$: owing to (5.5) and (5.7) there holds for any $u \in L^2(\Omega)$

$$\begin{aligned}\left\|(\overline{\mathsf{Q}}_l - \overline{\mathsf{Q}}_{l-1}) u\right\|_{L^2(\Omega)} &\leq \left\|(\overline{\mathsf{Q}}_l - \overline{\mathsf{Q}}_{l-1})(u - w)\right\|_{L^2(\Omega)} + \left\|(\overline{\mathsf{Q}}_l - \overline{\mathsf{Q}}_{l-1}) w\right\|_{L^2(\Omega)} \\ &\leq C\big(\|u - w\|_{L^2(\Omega)} + h_l^2 |w|_{H^2(\Omega)}\big) \quad \forall w \in H^2(\Omega) \ .\end{aligned}$$

Here and below the generic constants C may depend on shape regularity $\max\limits_{0 \leq l \leq L} \rho_{\widehat{\mathcal{M}}_l}$ and the (quasi-uniformity) constants in (3.3). We conclude

$$\left\|(\overline{\mathsf{Q}}_l - \overline{\mathsf{Q}}_{l-1}) u\right\|^2_{L^2(\Omega)} \leq C\, K(h_l^2, u)^2 \quad \forall u \in L^2(\Omega) \ , \tag{5.12}$$

which implies

$$\left|\overline{\mathsf{Q}}_0 u\right|^2_{H^1(\Omega)} + \sum_{l=1}^{L} h_l^{-2} \left\|(\overline{\mathsf{Q}}_l - \overline{\mathsf{Q}}_{l-1}) u\right\|^2_{L^2(\Omega)} \leq C \Big\{ |u|^2_{H^1(\Omega)} + \sum_{l=1}^{L} h_l^{-2} K(h_l^2, u) \Big\} \ . \tag{5.13}$$

Let $\widetilde{u} \in H^1(\mathbb{R}^3)$ be the Sobolev extension of u such that, with $C = C(\Omega) > 0$,

$$\widetilde{u}_{|\Omega} = u \quad \text{and} \quad |u|_{H^1(\mathbb{R}^3)} \leq C |u|_{H^1(\Omega)}.$$

Define the Fourier Transform of $\widetilde{u}$ by

$$\widehat{u}(\boldsymbol{\xi}) = \frac{1}{(2\pi)^{3/2}} \int_{\mathbb{R}^3} \widetilde{u}(\boldsymbol{x}) e^{-\imath \boldsymbol{x} \cdot \boldsymbol{\xi}} \, \mathrm{d}\boldsymbol{x}.$$

By the equivalent definition of Sobolev-norms on $\mathbb{R}^3$

$$|\widetilde{u}|^2_{H^i(\mathbb{R}^3)} \approx \int_{\mathbb{R}^3} |\boldsymbol{\xi}|^{2i} |\widehat{u}(\boldsymbol{\xi})|^2 \, \mathrm{d}\boldsymbol{\xi} \ , \quad i = 0, 1,$$

we have

$$\begin{aligned} K_{\mathbb{R}^3}(t,\widetilde{u})^2 &\leq C \inf_{w\in H^2(\mathbb{R}^3)} \int_{\mathbb{R}^3} \left\{ |\widehat{u}(\boldsymbol{\xi}) - \widehat{w}(\boldsymbol{\xi})|^2 + t^2|\boldsymbol{\xi}|^4 \, |\widehat{w}|^2 \right\} \mathrm{d}\boldsymbol{\xi} \\ &= C \int_{\mathbb{R}^3} \frac{t^2|\boldsymbol{\xi}|^4}{1+t^2|\boldsymbol{\xi}|^4} |\widehat{u}(\boldsymbol{\xi})|^2 \, \mathrm{d}\boldsymbol{\xi} \ , \end{aligned}$$

because the infimum is attained for $\widehat{w}(\boldsymbol{\xi}) = \widehat{u}(\boldsymbol{\xi})/(1+t^2|\boldsymbol{\xi}|^4)$. Since

$$\begin{aligned} K(t,u)^2 &= \inf_{w\in H^2(\Omega)} \left\{ \|u-w\|^2_{L^2(\Omega)} + t^2 \, |w|^2_{H^2(\Omega)} \right\} , \\ &= \inf_{w\in H^2(\mathbb{R}^3)} \left\{ \|u-w\|^2_{L^2(\Omega)} + t^2 \, |w|^2_{H^2(\Omega)} \right\} \leq K_{\mathbb{R}^3}(t,\widetilde{u})^2, \end{aligned}$$

we deduce that

$$\begin{aligned} \sum_{l=1}^{L} h_l^{-2} K(h_l^2, u)^2 &\leq C \sum_{l=1}^{L} \int_{\mathbb{R}^3} \frac{h_l^2|\boldsymbol{\xi}|^4}{1+h_l^4|\boldsymbol{\xi}|^4} |\widehat{u}(\boldsymbol{\xi})|^2 \, \mathrm{d}\boldsymbol{\xi} \\ &\leq C \sup_{\boldsymbol{\xi}\in\mathbb{R}^3} \left\{ \sum_{l=1}^{L} \frac{\theta^{2l}|\boldsymbol{\xi}|^2}{1+\theta^{4l}|\boldsymbol{\xi}|^4} \right\} \int_{\mathbb{R}^3} |\boldsymbol{\xi}|^2 |\widehat{u}(\boldsymbol{\xi})|^2 \, \mathrm{d}\boldsymbol{\xi} \\ &\leq C \, |\widehat{u}|^2_{H^1(\mathbb{R}^3)} \leq C |u|^2_{H^1(\Omega)}, \end{aligned} \tag{5.14}$$

where we have used assumption (3.3). The proof is finished by combining (5.13) and (5.14). ◻

Thanks to the particular design of the node→element–assignment underlying $\overline{\mathsf{Q}}_l$, the terms in the decomposition (5.10) turn out to be localized.

LEMMA 5.5. *For all $u_h \in V(\mathcal{M}_h)$ and $0 \leq l \leq j \leq L$,*

$$\overline{\mathsf{Q}}_j \mu_h = \mu_h \quad \text{in } \Omega \setminus \omega_{l+1}. \tag{5.15}$$

Proof. If $\boldsymbol{p} \in \overline{\mathcal{N}}(\widehat{\mathcal{M}}_j)$ and $\boldsymbol{p} \notin \omega_{l+1}$ (open set !), then $K_{\boldsymbol{p}} \not\subset \omega_{l+1}$ ($K_{\boldsymbol{p}} \in \widehat{\mathcal{M}}_j$). Recall that $K_{\boldsymbol{p}}$ was deliberately chosen such that there is $K \in \mathcal{M}_l$ with $K_{\boldsymbol{p}} \subset K$. Since u_h is linear on K, the same holds for $K_{\boldsymbol{p}}$ and (5.1) guarantees

$$(\overline{\mathsf{Q}}_j u_h)(\boldsymbol{p}) = u_h(\boldsymbol{p}) \ .$$

When restricted to $\Omega \setminus \omega_{l+1}$, the mesh $\widehat{\mathcal{M}}_j$ is a refinement of $\mathcal{M}_h$. Hence, agreement of the $\mathcal{M}_h$-piecewise linear function u_h with $\overline{\mathsf{Q}}_j u_h$ in all nodes of $\widehat{\mathcal{M}}_j$ outside ω_{l+1} implies $\overline{\mathsf{Q}}_j u_{h|\Omega\setminus\omega_{l+1}} = u_{h|\Omega\setminus\omega_{l+1}}$. ◻

Consequently, for any $u_h \in V(\mathcal{M}_h)$, outside ω_l both $\overline{\mathsf{Q}}_l u_h$ and $\overline{\mathsf{Q}}_{l-1} u_h$ agree with u_h.

COROLLARY 5.6. *For any $u_h \in V(\mathcal{M}_h)$ and $1 \leq l \leq L$,*

$$\operatorname{supp}((\overline{\mathsf{Q}}_l - \overline{\mathsf{Q}}_{l-1})u_h) \subset \overline{\omega}_l \ .$$

In other words, the components of (5.10) are localized inside refined regions of Ω. In light of the definition (4.1) of the refinement zones, we also find

$$(\overline{\mathsf{Q}}_l - \overline{\mathsf{Q}}_{l-1})u_h \in \overline{V}(\mathcal{M}_l)\,! \tag{5.16}$$

However, having used $\overline{\mathsf{Q}}_l$ we cannot expect the splitting to match potential homogeneous Dirichlet boundary conditions. This can be remedied using Oswald's trick [34, Cor. 30]. We fix $u_h \in V(\mathcal{M}_h)$ and abbreviate $u_0 = \overline{\mathsf{Q}}_0 u_h \in \overline{V}(\mathcal{M}_0)$, $u_l := (\overline{\mathsf{Q}}_l - \overline{\mathsf{Q}}_{l-1})u_h \in \overline{V}(\mathcal{M}_l)$, $l \geq 1$. Then, we consider the partial sums

$$\overline{s}_l := \sum_{j=0}^{l} u_j \in \overline{V}(\mathcal{M}_l) \quad l \geq 0\,. \tag{5.17}$$

Flatly dropping those basis functions in $\overline{\mathfrak{B}}_V(\mathcal{M}_l)$ that belong to vertices in $\overline{\Gamma_D}$ in the representation of $\overline{s}_l$ we arrive at $s_l \in V(\mathcal{M}_l) \in H^1_{\Gamma_D}(\Omega)$.

Due to Cor. 5.6, we observe that

$$\overline{s}_l \text{ and } \overline{s}_{l-1} \text{ agree on } \Omega \setminus \omega_l. \tag{5.18}$$

Hence, away from $\overline{\omega}_l \cap \overline{\Gamma_D}$ the same basis contribution are removed from both functions when building s_l and s_{l-1}, respectively. This permits us to conclude

$$s_l \text{ and } s_{l-1} \text{ agree on } \Omega \setminus \omega_l. \tag{5.19}$$

Putting it differently,

$$\operatorname{supp}(s_l - s_{l-1}) \subset \omega_l\,. \tag{5.20}$$

Hence, for all $1 \leq l \leq L$ we can estimate

$$\begin{aligned} \|s_l - s_{l-1}\|_{L^2(\Omega)} &= \|s_l - s_{l-1}\|_{L^2(\omega_l)} \\ &\leq \|s_l - \overline{s}_l\|_{L^2(\omega_l)} + \|s_{l-1} - \overline{s}_{l-1}\|_{L^2(\omega_l)} + \|u_l\|_{L^2(\omega_l)}\,. \end{aligned} \tag{5.21}$$

The benefit of zeroing in on ω_l is that on this subdomain $\overline{s}_l$ has the same "uniform scale" h_l as u_l. Thus, repeated application of uniform L^2-stability estimates for basis representations and elementary Cauchy-Schwarz inequalities make possible the estimates (for arbitrary $0 < \epsilon < \frac{1}{2}$)

$$\begin{aligned} \|s_l - \overline{s}_l\|^2_{L^2(\omega_l)} &\leq C h_l^3 \sum_{\boldsymbol{p} \in \mathcal{N}(\Gamma_l)} \overline{s}_l(\boldsymbol{p})^2 \leq C h_l \left\| \overline{s}_{l|\partial\Omega} \right\|^2_{L^2(\Gamma_l)} = C h_l \left\| \sum_{j=0}^{L} u_j - \sum_{j=0}^{l} u_j \right\|^2_{L^2(\Gamma_l)} \\ &\leq C h_l \Big(\sum_{j=l+1}^{L} \|u_j\|_{L^2(\Gamma_l)} \Big)^2 \leq C h_l \Big(\sum_{j=l+1}^{L} h_j^{-\frac{1}{2}} \|u_j\|_{L^2(\omega_l)} \Big)^2 \\ &\leq C h_l \cdot \sum_{j=l+1}^{L} h_j^{1-2\epsilon} \cdot \sum_{j=l+1}^{L} h_j^{2\epsilon-2} \|u_j\|^2_{L^2(\omega_l)} \\ &\leq C h_l^{2-2\epsilon} \cdot \sum_{j=l+1}^{L} h_j^{2\epsilon-2} \|u_j\|^2_{L^2(\omega_l)}\,. \end{aligned}$$

Here the set $\mathcal{N}(\Gamma_l)$ comprises the nodes of $\overline{\mathcal{N}}(\widehat{\mathcal{M}}_l)$ that lie on $\overline{\omega}_l \cap \overline{\Gamma_D}$ and we make heavy use of the geometric decay of h_l. The latter also yields

$$\begin{aligned}\sum_{l=1}^{L} h_l^{-2} \|s_l - \overline{s}_l\|^2_{L^2(\omega_l)} &\leq C \sum_{l=1}^{L} h_l^{-2\epsilon} \sum_{j=l+1}^{L} h_j^{2\epsilon-2} \|u_j\|^2_{L^2(\omega_l)} \\ &= C \sum_{j=2}^{L} \left(\sum_{l=1}^{j} h_l^{-2\epsilon} \right) h_j^{-2+2\epsilon} \|u_j\|^2_{L^2(\omega_l)} \\ &\leq C \sum_{j=2}^{L} h_j^{-2} \|u_j\|^2_{L^2(\Omega)} \leq C |u_h|^2_{H^1(\Omega)} ,\end{aligned}$$

by virtue of Lemma 5.4. Except for the last line, all constants only depend on $\rho_{\widehat{\mathcal{M}}_l}$ and the constants in (3.3). Merging the last estimate with (5.21) gives us

$$\sum_{l=1}^{L} h_l^{-2} \|s_l - s_{l-1}\|^2_{L^2(\Omega)} \leq C |u_h|^2_{H^1(\Omega)} . \tag{5.22}$$

Thus, in light of (5.20) and the following identity

$$s_0 + \sum_{l=1}^{L} (s_l - s_{l-1}) = s_L = \overline{s}_L = u_h,$$

we have accomplished the proof of the following theorem:

THEOREM 5.7. *For any $u_h \in V(\mathcal{M}_h)$ we can find $u_l \in V(\mathcal{M}_l)$ such that*

$$u_h = \sum_{l=0}^{L} u_l, \qquad \operatorname{supp}(u_l) \subset \overline{\omega}_l , \tag{5.23}$$

and

$$|u_0|^2_{H^1(\Omega)} + \sum_{l=1}^{L} h_l^{-2} \|u_l\|^2_{L^2(\Omega)} \leq C |u_h|^2_{H^1(\Omega)} ,$$

with $C > 0$ independent of L.

Notice that in combination with the L^2-stability (2.6) of nodal bases and inverse inequalities, this theorem asserts an L-uniform estimate of the form (4.6) for the splitting (4.10) w.r.t. the energy norm $|\cdot|_{H^1(\Omega)}$. From (5.23) it is clear that the basis functions admitted in (4.10) can represent the functions u_l of Thm. 5.7.

REMARK 5.8. *It is interesting to note that, in contrast to other analyses [1, 9], the above proof does not impose restrictions on the ratios of sizes of adjacent elements. This becomes relevant for refinement with hanging nodes: our theory for the $H^1(\Omega)$-case can cope with an arbitrary number of hanging nodes on an active edge.*

5.3. Helmholtz-type decompositions. Helmholtz-type decompositions have emerged as a powerful tool for answering questions connected with $\boldsymbol{H}(\mathbf{curl}, \Omega)$. In particular, they have paved the way for a rigorous multigrid theory for $\boldsymbol{H}(\mathbf{curl}, \Omega)$-elliptic problems [14, 21, 24, 26–28, 36]. We refer to [25, Sect. 2.4] for more information.

We will need a very general version provided by the following theorem.

THEOREM 5.9. *Let Ω meet the requirements stated in Sect. 1. Then, for any $\mathbf{v} \in \boldsymbol{H}_{\Gamma_D}(\mathbf{curl}, \Omega)$, there exists a $p \in H^1_{\Gamma_D}(\Omega)$ and $\boldsymbol{\Psi} \in (H^1_{\Gamma_D}(\Omega))^3$ such that*

$$\mathbf{v} = \nabla p + \boldsymbol{\Psi}, \tag{5.24}$$

$$|p|_{H^1(\Omega)} \leq C\|\mathbf{v}\|_{\boldsymbol{H}(\mathbf{curl},\Omega)}, \quad \|\boldsymbol{\Psi}\|_{H^1(\Omega)} \leq C\|\,\mathbf{curl}\,\mathbf{v}\|_{L^2(\Omega)}, \tag{5.25}$$

where the constant C only depends on Ω.

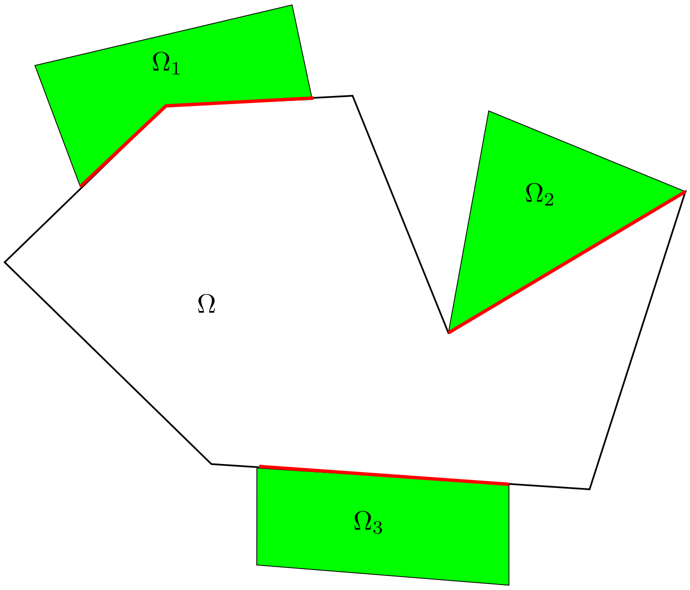

FIG. 5.2. *Buffer zones attached to connected components of (red) Dirichlet boundary part Γ_D*

Proof. Given $\mathbf{u} \in \boldsymbol{H}_{\Gamma_D}(\mathbf{curl}, \Omega)$, we define $\widetilde{\mathbf{u}} \in \boldsymbol{H}(\mathbf{curl}, \widetilde{\Omega})$, $\widetilde{\Omega} :=$ interior$(\overline{\Omega} \cup \overline{\Omega}_1 \cup \overline{\Omega}_2 \cup \dots)$ (see Sect. 1 and Fig. 5.2 for the meaning of Ω_i), by

$$\widetilde{\mathbf{u}}(\boldsymbol{x}) = \begin{cases} \mathbf{u}(\boldsymbol{x}) & \text{for } \boldsymbol{x} \in \Omega\ , \\ 0 & \text{for } \boldsymbol{x} \in \Omega_i \text{ for some } i\ . \end{cases} \tag{5.26}$$

Notice that the tangential components of $\widetilde{\mathbf{u}}$ are continuous across $\partial\Omega$, which ensures $\widetilde{\mathbf{u}} \in \boldsymbol{H}(\mathbf{curl}, \widetilde{\Omega})$. Then extend $\widetilde{\mathbf{u}}$ to $\overline{\mathbf{u}} \in \boldsymbol{H}(\mathbf{curl}, \mathbb{R}^3)$, see [13].

Since $\mathbf{curl}\,\overline{\mathbf{u}} \in \boldsymbol{H}(\mathrm{div}\,0, \mathbb{R}^3)$, Fourier techniques [20] yield a $\boldsymbol{\Phi} \in (H^1(\mathbb{R}^3))^3$ that fulfills

$$\mathbf{curl}\,\boldsymbol{\Phi} = \mathbf{curl}\,\overline{\mathbf{u}}\ , \quad \|\boldsymbol{\Phi}\|_{H^1(\mathbb{R}^3)} \leq C\,\|\mathbf{curl}\,\overline{\mathbf{u}}\|_{L^2(\mathbb{R}^3)}\ , \tag{5.27}$$

with $C = C(\Omega) > 0$. As a consequence

$$\mathbf{curl}(\overline{\mathbf{u}} - \boldsymbol{\Phi}) = 0 \quad \Rightarrow \quad \overline{\mathbf{u}} - \boldsymbol{\Phi} = \mathrm{grad}\, q \quad \text{in } \mathbb{R}^3\ . \tag{5.28}$$

On every Ω_i, by definition $\overline{\mathbf{u}} = 0$, which implies $q_{|\Omega_i} \in H^2(\Omega_i)$. As the attached domains Ω_i are well separated Lipschitz domains, see Fig. 5.2, the H^2-extension of $q_{|\bigcup_i \Omega_i}$ to $\overline{q} \in H^2(\mathbb{R}^3)$ is possible. Moreover, it satisfies

$$\|\overline{q}\|_{H^2(\mathbb{R}^3)} \leq C\|q\|_{H^2(\bigcup_i \Omega_i)} \leq C\|\boldsymbol{\Phi}\|_{H^1(\mathbb{R}^3)} \leq \|\mathbf{curl}\,\mathbf{u}\|_{L^2(\Omega)}\ . \tag{5.29}$$

$$\overline{\mathbf{u}} = \mathbf{\Phi} - \operatorname{grad}\overline{q} + \operatorname{grad}(q + \overline{q}) \ . \tag{5.30}$$

Finally, set $\mathbf{\Psi} := (\mathbf{\Phi} - \operatorname{grad}\overline{q})_{|\Omega}$, $p := q + \overline{q}$, and observe

$$\|\mathbf{\Psi}\|_{H^1(\Omega)} \leq \|\mathbf{\Phi}\|_{H^1(\mathbb{R}^3)} + \|\overline{q}\|_{H^2(\mathbb{R}^3)} \leq C \left\|\mathbf{curl}\,\mathbf{u}\right\|_{L^2(\Omega)} \ . \tag{5.31}$$

The constants may depend on Ω, Γ_D, and the chosen Ω_i. ◻

The stable Helmholtz-type decomposition (5.24) immediately suggests the following idea: when given $\mathbf{v}_h \in \mathbf{U}(\mathcal{M}_h)$, first split it according to (5.24) and then attack both components by the uniformly H^1-stable local multilevel decompositions explored in the previous section. Alas, the idea is flawed, because neither of the terms in (5.24) is guaranteed to be a finite element function, even if this holds for $\mathbf{v}_h$.

Fortunately, the idea can be mended by building a purely discrete counterpart of (5.24) as in [28, Lemma 5.1]. For the sake of completeness we also elaborate the proof below.

However, to accommodate nonconforming meshes in our theory, we have to rule out extreme jumps of local meshwidth. For the sake of simplicity, we make the following assumption for the rest of this section:

Assumption 5.9.1. *Any edge of $\mathcal{M}_h$ may contain at most one hanging node.*

As a consequence, there exists a constant $C > 0$ independent of the mesh such that

$$\forall K_1, K_2 \in \mathcal{M}_h,\ \overline{K}_1 \bigcap \overline{K}_2 \neq \emptyset : \quad C^{-1} h_{K_1} \leq h_{K_2} \leq C h_{K_1} \ . \tag{5.32}$$

Moreover, given that the mesh $\mathcal{M}$ complies with Ass. 5.9.1, the assertion of Lemma 2.1 remains valid for the interpolation onto $\mathbf{U}(\mathcal{M})$. This can be concluded from local considerations. zeroing on a situation, for which a 2D analogue is depicted in Fig. 5.3.

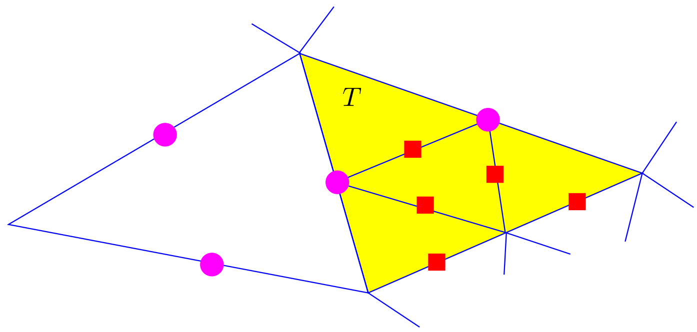

Fig. 5.3. *subdivided triangle (yellow) with hanging nodes. The magenta disks represent "coarse" active edges, the red squares "fine" active edges.*

Write T for a subdivided tetrahedron, with edges carrying hanging nodes. We define $\mathbf{U}_T := \mathbf{U}(\mathcal{M})_{|T}$ and, temporarily, $\mathbf{\Pi}_h$ to be the corresponding edge interpolation operator, *cf.* (2.5). In addition, let $\mathbf{\Pi}_T$ be the edge interpolation onto the local edge element space $\mathbf{U}(T)$. Simple affine transformation techniques establish that

$$|\mathbf{\Pi}_h \mathbf{u}|_{H^1(T)} \leq C |\mathbf{u}|_{H^1(T)} \quad \forall \mathbf{u} \in \{\mathbf{v} \in (H^1(T))^3 : \ \mathbf{curl}\,\mathbf{u} \in \mathbf{curl}\,\mathbf{U}_T\} \ , \tag{5.33}$$

with $C > 0$ only depending on the shape regularity of T. Thus, by using Lemma 2.1 and (5.33) and because $\mathbf{\Pi}_h \circ \mathbf{\Pi}_T = \mathbf{\Pi}_T$,

$$\|\mathbf{u} - \mathbf{\Pi}_h \mathbf{u}\|_{L^2(T)} \leq \|\mathbf{u} - \mathbf{\Pi}_T \mathbf{u}\|_{L^2(T)} + C \left\|\mathbf{u} - \mathbf{\Pi}_T \mathbf{u}\right\|_{L^2(T)} \leq C h_T |\mathbf{u}|_{H^1(T)} \ ,$$

for all $\mathbf{u} \in \{\mathbf{v} \in (H^1(T))^3 : \ \mathbf{curl}\,\mathbf{u} \in \mathbf{curl}\,\mathbf{U}_T\}$. Therefore, without further explanation, we will use the estimate of Lemma 2.1 for meshes with hanging nodes, too.

Hanging nodes can be removed by invoking so-called green refinements [7], see Fig. 5.4. This will create another conforming mesh $\mathcal{T}_h$, which satisfies $\mathcal{M}_h \prec \mathcal{T}_h$ and

$$\forall K \in \mathcal{T}_h : \quad \exists K' \in \mathcal{M}_h : \quad K \subset K' \quad \wedge \quad h_{K'} \leq C h_K \ , \tag{5.34}$$

with $C > 0$ only depending on the shape regularity measure $\rho_{\mathcal{M}_h}$. In other words, $\mathcal{M}_h$ and $\mathcal{T}_h$ have about the same local resolution: writing $h_{\mathcal{M}}$ and $h_{\mathcal{T}}$ for the respective locally constant meshwidth functions, we find

$$\exists C = C(\rho_{\mathcal{M}_h}) > 0 : \quad C^{-1} h_{\mathcal{M}} \leq h_{\mathcal{T}} \leq C h_{\mathcal{M}} \quad \text{a.e. in } \Omega \ . \tag{5.35}$$

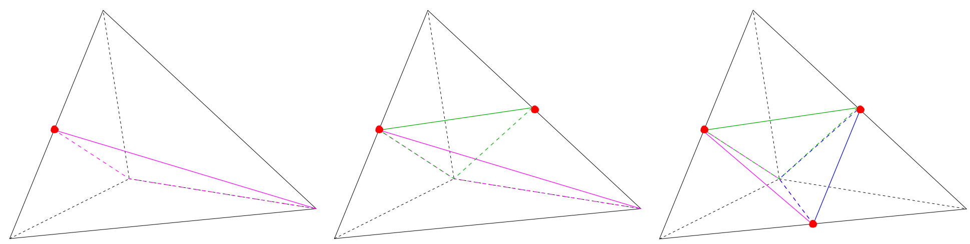

FIG. 5.4. *Green refinements of a tetrahedron with hanging nodes (marked red).*

The close relationship between local meshwidths implies uniform continuity of finite element interpolations back and forth between $\mathcal{M}_h$ and $\mathcal{T}_h$. In particular, standard local scaling arguments confirm the existence of a constant $C = C(\rho_{\mathcal{M}_h}) > 0$ such that

$$\left\| h_{\mathcal{M}}^k \mathbf{\Pi}_h \mathbf{w}_h \right\|_{L^2(\Omega)} \leq C \left\| h_{\mathcal{T}}^k \mathbf{w}_h \right\|_{L^2(\Omega)} \quad \forall \mathbf{w}_h \in \mathbf{U}(\mathcal{T}_h), \ k = 0, -1 \ , \tag{5.36}$$

$$\left\| h_{\mathcal{M}}^{-1} (Id - \mathcal{I}_h) \mathbf{\Psi}_h \right\|_{L^2(\Omega)} \leq C |\mathbf{\Psi}_h|_{H^1(\Omega)} \quad \forall \mathbf{\Psi}_h \in (V(\mathcal{T}_h))^3 \ , \tag{5.37}$$

where $\mathcal{I}_h$ is componentwise linear interpolation onto $(V(\mathcal{M}_h))^3$.

LEMMA 5.10. *For any $\mathbf{v}_h \in \mathbf{U}(\mathcal{M}_h)$, there is $\mathbf{\Psi}_h \in (V(\mathcal{M}_h))^3$, $p_h \in V(\mathcal{M}_h)$, and $\widetilde{\mathbf{v}}_h \in \mathbf{U}(\mathcal{M}_h)$ such that*

$$\mathbf{v}_h = \widetilde{\mathbf{v}}_h + \mathbf{\Pi}_h \mathbf{\Psi}_h + \nabla p_h \ , \tag{5.38}$$

$$\|p_h\|_{H^1(\Omega)} \leq C \|\mathbf{v}_h\|_{\boldsymbol{H}(\mathbf{curl},\Omega)} \ , \tag{5.39}$$

$$\left\| h^{-1} \widetilde{\mathbf{v}}_h \right\|_{L^2(\Omega)} + \|\mathbf{\Psi}_h\|_{H^1(\Omega)} \leq C \|\mathbf{curl}\,\mathbf{v}_h\|_{L^2(\Omega)} \ , \tag{5.40}$$

where the constant C only depends on Ω, Γ_D, and the shape regularity of $\mathcal{M}_h$.

Proof. (*cf.* [28, Lemma 5.1]) Initially, we confine ourselves to conforming meshes. We fix a $\mathbf{v}_h \in \mathbf{U}(\mathcal{M}_h)$ and use the stable regular decomposition of Thm. 5.9 to split it according to

$$\mathbf{v}_h = \mathbf{\Psi} + \operatorname{grad} p \ , \quad \mathbf{\Psi} \in (H^1_{\Gamma_D}(\Omega))^3 \ , \quad p \in H^1_{\Gamma_D}(\Omega) \ . \tag{5.41}$$

We have already known that the functions $\mathbf{\Psi}$ and p satisfy

$$\|\mathbf{\Psi}\|_{H^1(\Omega)} \leq C \|\mathbf{curl}\,\mathbf{v}_h\|_{L^2(\Omega)} \quad , \quad \|\operatorname{grad} p\|_{L^2(\Omega)} \leq C \|\mathbf{v}_h\|_{\boldsymbol{H}(\mathbf{curl},\Omega)} \ , \tag{5.42}$$

with constants only depending on Ω and Γ_D.

Next, note that in (5.41) $\mathbf{curl}\,\boldsymbol{\Psi} = \mathbf{curl}\,\mathbf{v}_h \in \mathbf{curl}\,\mathbf{U}(\mathcal{M}_h)$, and, owing to Lemma 2.1, $\boldsymbol{\Pi}_h\boldsymbol{\Psi}$ is well defined. Further, a commuting diagram property together with Lemma 2.3 implies

$$\mathbf{curl}(Id - \boldsymbol{\Pi}_h)\boldsymbol{\Psi} = 0 \quad \Rightarrow \quad \exists q \in H^1_{\Gamma_D}(\Omega): \quad (Id - \boldsymbol{\Pi}_h)\boldsymbol{\Psi} = \operatorname{grad} q\,. \tag{5.43}$$

The estimate of Lemma 2.1 together with (5.42) yields

$$\left\|h^{-1}\operatorname{grad} q\right\|_{L^2(\Omega)} = \left\|h^{-1}(Id - \boldsymbol{\Pi}_h)\boldsymbol{\Psi}\right\|_{L^2(\Omega)} \le C|\boldsymbol{\Psi}|_{H^1(\Omega)} \le C\left\|\mathbf{curl}\,\mathbf{v}_h\right\|_{L^2(\Omega)}\,. \tag{5.44}$$

In order to push $\boldsymbol{\Psi}$ into a finite element space, a quasi-interpolation operator $\mathsf{Q}_h : (L^2(\Omega))^3 \mapsto (V(\mathcal{M}_h))^3$ is the right tool. We simply get it from componentwise application of an operator according to Def. 5.1 where any node→element–assignment will do. Thus, we can define the terms in the decomposition (5.38) as

$$\widetilde{\mathbf{v}}_h := \boldsymbol{\Pi}_h(\boldsymbol{\Psi} - \mathsf{Q}_h\boldsymbol{\Psi}) \in \mathbf{U}(\mathcal{M}_h)\,, \tag{5.45}$$

$$\boldsymbol{\Psi}_h := \mathsf{Q}_h\boldsymbol{\Psi} \in (V(\mathcal{M}_h))^3\,, \tag{5.46}$$

$$\operatorname{grad} p_h := \operatorname{grad}(p+q)\,, \quad p_h \in V(\mathcal{M}_h)\,. \tag{5.47}$$

Indeed, $\operatorname{grad}(p+q) \in \mathbf{U}(\mathcal{M}_h)$ such that $p+q \in V(\mathcal{M}_h)$. The stability of the decomposition (5.38) can be established as follows: first, make use of Lemma 2.1 and (5.7) to obtain, with $C = C(\rho_{\mathcal{M}_h}) > 0$,

$$\begin{aligned}
\left\|h^{-1}\widetilde{\mathbf{v}}_h\right\|_{L^2(\Omega)} &\le \left\|h^{-1}(Id - \boldsymbol{\Pi}_h)(\boldsymbol{\Psi} - \mathsf{Q}_h\boldsymbol{\Psi})\right\|_{L^2(\Omega)} + \left\|h^{-1}(Id - \mathsf{Q}_h)\boldsymbol{\Psi}\right\|_{L^2(\Omega)} \\
&\le C|(Id - \mathsf{Q}_h)\boldsymbol{\Psi}|_{H^1(\Omega)} + |\boldsymbol{\Psi}|_{H^1(\Omega)} \\
&\le C|\boldsymbol{\Psi}|_{H^1(\Omega)} \le C\left\|\mathbf{curl}\,\mathbf{v}_h\right\|_{L^2(\Omega)}\,.
\end{aligned}$$

Due to the definition (5.46), the next estimate is a simple consequence of (5.6) and Thm. 5.9

$$\|\boldsymbol{\Psi}_h\|_{H^1(\Omega)} \le C\|\boldsymbol{\Psi}\|_{H^1(\Omega)} \le C\left\|\mathbf{curl}\,\mathbf{v}_h\right\|_{L^2(\Omega)}\,. \tag{5.48}$$

Finally, the estimates established so far plus the triangle inequality yield

$$\|\operatorname{grad} p_h\|_{L^2(\Omega)} \le C\left\|\mathbf{v}_h\right\|_{\boldsymbol{H}(\mathbf{curl},\Omega)}\,. \tag{5.49}$$

Next, we tackle meshes with hanging nodes satisfying Assumption 5.9.1. Let an auxiliary conforming mesh $\mathcal{T}_h$ be constructed as above. Since $\mathbf{v}_h \in \mathbf{U}(\mathcal{M}_h) \subset \mathbf{U}(\mathcal{T}_h)$, by the above arguments, there is $\widehat{\boldsymbol{\Psi}}_h \in (V(\mathcal{T}_h))^3$, $q_h \in V(\mathcal{T}_h)$, and $\mathbf{w}_h \in \mathbf{U}(\mathcal{T}_h)$ such that

$$\mathbf{v}_h = \mathbf{w}_h + \boldsymbol{\Pi}_{\mathcal{T}_h}\widehat{\boldsymbol{\Psi}}_h + \nabla q_h\,, \tag{5.50}$$

$$\|q_h\|_{H^1(\Omega)} \le C\left\|\mathbf{v}_h\right\|_{\boldsymbol{H}(\mathbf{curl},\Omega)}\,, \tag{5.51}$$

$$\left\|h^{-1}\mathbf{w}_h\right\|_{L^2(\Omega)} + \left\|\widehat{\boldsymbol{\Psi}}_h\right\|_{H^1(\Omega)} \le C\left\|\mathbf{curl}\,\mathbf{v}_h\right\|_{L^2(\Omega)}\,, \tag{5.52}$$

where $\boldsymbol{\Pi}_{\mathcal{T}_h}$ is the interpolation operator onto $\mathbf{U}(\mathcal{T}_h)$. Using the commuting diagram and Lemma 2.2, we have

$$\begin{aligned}
\mathbf{v}_h &= \boldsymbol{\Pi}_h\mathbf{w}_h + \boldsymbol{\Pi}_h\boldsymbol{\Pi}_{\mathcal{T}_h}\widehat{\boldsymbol{\Psi}}_h + \boldsymbol{\Pi}_h\nabla q_h = \boldsymbol{\Pi}_h\mathbf{w}_h + \boldsymbol{\Pi}_h\widehat{\boldsymbol{\Psi}}_h + \nabla(\mathcal{I}_h q_h) \\
&= \boldsymbol{\Pi}_h\mathbf{w}_h + \boldsymbol{\Pi}_h(Id - \mathcal{I}_h)\widehat{\boldsymbol{\Psi}}_h + \boldsymbol{\Pi}_h\mathcal{I}_h\widehat{\boldsymbol{\Psi}}_h + \nabla(\mathcal{I}_h q_h)\,.
\end{aligned}$$

Setting $\widetilde{\mathbf{v}}_h = \mathbf{\Pi}_h \mathbf{w}_h + \mathbf{\Pi}_h(Id - \mathcal{I}_h)\widehat{\mathbf{\Psi}}_h$, (5.36) and (5.37) together with (5.35) yield

$$\begin{aligned} \left\| h^{-1}\widetilde{\mathbf{v}}_h \right\|_{L^2(\Omega)} &\leq \left\| h^{-1}\mathbf{\Pi}_h \mathbf{w}_h \right\|_{L^2(\Omega)} + \left\| h^{-1}(Id - \mathcal{I}_h)\widehat{\mathbf{\Psi}}_h \right\|_{L^2(\Omega)} \\ &\leq \left\| h_{\mathcal{T}}^{-1}\mathbf{w}_h \right\|_{L^2(\Omega)} + \left| \widehat{\mathbf{\Psi}}_h \right|_{H^1(\Omega)} . \end{aligned} \tag{5.53}$$

In addition, we may choose $p_h = \mathcal{I}_h q_h$ and $\mathbf{\Psi}_h := \mathcal{I}_h \widehat{\mathbf{\Psi}}_h$ and easily see

$$\begin{aligned} \|p_h\|_{H^1(\Omega)} &\leq \|q_h\|_{H^1(\Omega)} \leq C \|\mathbf{v}_h\|_{\boldsymbol{H}(\mathbf{curl},\Omega)} , \\ \|\mathbf{\Psi}_h\|_{H^1(\Omega)} &\leq \left\| \widehat{\mathbf{\Psi}}_h \right\|_{H^1(\Omega)} \leq C \|\mathbf{curl}\, \mathbf{v}_h\|_{L^2(\Omega)} . \end{aligned}$$

This finishes the proof also for nonconforming meshes. ◻

5.4. Local multilevel splitting of $\mathbf{U}(\mathcal{M}_h)$. With the discrete Helmholz-type decomposition of Lemma 5.10 at our disposal, we can now tackle its piecewise linear and continuous components with Thm. 5.7.

LEMMA 5.11. *For any $\mathbf{v}_h \in \mathbf{U}(\mathcal{M}_h)$, there exists a constant C only depending on the domain, the Dirichlet boundary part Γ_D, the shape regularity of the meshes $\mathcal{M}_l$, $\widehat{\mathcal{M}}_l$, $0 \leq l \leq L$, and the constants in* (3.3)*, such that*

$$\mathbf{v}_h = \sum_{l=0}^{L} \Big(\mathbf{v}_l + \nabla p_l \Big), \quad \mathbf{v}_l \in \operatorname{Span}\left\{ \mathfrak{B}_{\mathbf{U}}^l \right\},\ p_l \in \operatorname{Span}\left\{ \mathfrak{B}_V^l \right\} , \tag{5.54}$$

and

$$\|\mathbf{v}_0\|^2_{\boldsymbol{H}(\mathbf{curl},\Omega)} + |p_0|^2_{H^1(\Omega)} + \sum_{l=1}^{L} h_l^{-2} \Big(\|\mathbf{v}_l\|^2_{L^2(\Omega)} + \|p_l\|^2_{L^2(\Omega)} \Big) \leq C \|\mathbf{v}_h\|^2_{\boldsymbol{H}(\mathbf{curl},\Omega)} , \tag{5.55}$$

where $\mathfrak{B}_V^l$ and $\mathfrak{B}_{\mathbf{U}}^l$ are defined in (4.9).

Proof. We start from the discrete Helmholtz-type decomposition of $\mathbf{v}_h$ in (5.38):

$$\mathbf{v}_h = \widetilde{\mathbf{v}}_h + \mathbf{\Pi}_h \mathbf{\Psi}_h + \nabla p_h, \quad \mathbf{\Psi}_h \in (V(\mathcal{M}_h))^3,\ p_h \in V(\mathcal{M}_h),\ \widetilde{\mathbf{v}}_h \in \mathbf{U}(\mathcal{M}_h).$$

We apply the result of Thm. 5.7 about the existence of stable local multilevel splittings of $V(\mathcal{M}_h)$ componentwise to $\mathbf{\Psi}_h$: this gives

$$\mathbf{\Psi}_h = \sum_{l=0}^{L} \mathbf{\Psi}_l , \quad \mathbf{\Psi}_l \in \operatorname{Span}\left\{ \mathfrak{B}_V^l \right\}^3 , \tag{5.56}$$

$$|\mathbf{\Psi}_0|^2_{H^1(\Omega)} + \sum_{l=1}^{L} h_l^{-2} \|\mathbf{\Psi}_l\|^2_{L^2(\Omega)} \leq C |\mathbf{\Psi}_h|^2_{H^1(\Omega)} . \tag{5.57}$$

Observe that the functions $\mathbf{\Psi}_l$ do not belong to $\mathbf{U}(\mathcal{M}_l)$. Thus, we target them with edge element interpolation operators $\mathbf{\Pi}_l$ onto $\mathbf{U}(\mathcal{M}_l)$, see (2.5), and obtain the splitting described in Lemma 2.2:

$$\mathbf{\Psi}_l = \mathbf{\Pi}_l \mathbf{\Psi}_l + \nabla w_l , \quad w_l \in \widetilde{V}_2(\mathcal{M}_l) . \tag{5.58}$$

The gradient terms introduced by (5.58) are well under control: writing $s_h := \sum_{l=0}^{L} w_l$, the L^2-stability of (5.58), see Lemma 2.2, yields

$$\|\mathbf{\Pi}_l \mathbf{\Psi}_l\|_{L^2(\Omega)} \leq C \|\mathbf{\Psi}_l\|_{L^2(\Omega)} \ ,$$

$$|s_h|^2_{H^1(\Omega)} \leq C\Big(\sum_{l=0}^{L} \|\mathbf{\Psi}_l\|_{L^2(\Omega)}\Big)^2 \leq C \sum_{l=0}^{L} h_l^2 \cdot \sum_{l=0}^{L} h_l^{-2} \|\mathbf{\Psi}_l\|^2_{L^2(\Omega)} \overset{(5.57)}{\leq} C|\mathbf{\Psi}_h|^2_{H^1(\Omega)} \ .$$

Because of $\mathbf{curl}\,\mathbf{\Pi}_0\mathbf{\Psi}_0 = \mathbf{curl}\,\mathbf{\Psi}_0$, we infer from (5.57)

$$\|\mathbf{\Pi}_0\mathbf{\Psi}_0\|^2_{\boldsymbol{H}(\mathbf{curl},\Omega)} + \sum_{l=1}^{L} h_l^{-2} \|\mathbf{\Pi}_l\mathbf{\Psi}_l\|^2_{L^2(\Omega)} \leq C|\mathbf{\Psi}_h|^2_{H^1(\Omega)} \ . \tag{5.59}$$

Above and throughout the remainder of the proof, constants are independent of L.

By the projector property $\mathbf{\Pi}_h \circ \mathbf{\Pi}_l = \mathbf{\Pi}_l$, $l = 0, \ldots, L$, and the commuting diagram property (2.8), we arrive at

$$\mathbf{v}_h = \widetilde{\mathbf{v}}_h + \sum_{l=0}^{L} \mathbf{\Pi}_l \mathbf{\Psi}_l + \operatorname{grad}(\mathcal{I}_h s_h + p_h) \ , \tag{5.60}$$

where $\mathcal{I}_h$ is the nodal linear interpolation operator onto $V(\mathcal{M}_h)$. Recall (2.17) to see that

$$|\mathcal{I}_h s_h + p_h|_{H^1(\Omega)} \leq C|s_h|_{H^1(\Omega)} + |p_h|_{H^1(\Omega)} \leq C \|\mathbf{v}_h\|_{\boldsymbol{H}(\mathbf{curl},\Omega)} \ .$$

The local multilevel splitting of $\mathcal{I}_h s_h + p_h$ according to Thm. 5.7 gives

$$\mathcal{I}_h s_h + p_h = \sum_{l=0}^{L} p_l \ , \quad p_l \in \operatorname{Span}\left\{\mathfrak{B}_V^l\right\} \ , \tag{5.61}$$

$$|p_0|^2_{H^1(\Omega)} + \sum_{l=1}^{L} h_l^{-2} \|p_l\|^2_{L^2(\Omega)} \leq C|\mathcal{I}_h s_h + p_h|^2_{H^1(\Omega)} \leq C \|\mathbf{v}_h\|^2_{\boldsymbol{H}(\mathbf{curl},\Omega)} \ . \tag{5.62}$$

Still, the contribution $\widetilde{\mathbf{v}}_h$ does not yet match (4.11). The idea is to distribute $\widetilde{\mathbf{v}}_h$ to the $\mathbf{\Pi}_l\mathbf{\Psi}_l$ by scale separation. To that end, we assign a level to each active edge of $\mathcal{M}_h$

$$\ell(E) := \min\{\ell(K) : \ K \in \mathcal{M}_h, \ E \subset \overline{K}\} \ , \quad E \in \mathcal{E}(\mathcal{M}_h) \ . \tag{5.63}$$

Thus, we distinguish parts of $\widetilde{\mathbf{v}}_h$ on different levels: given the basis representation

$$\widetilde{\mathbf{v}}_h = \sum_{E \in \mathcal{E}(\mathcal{M}_h)} \alpha_E \mathbf{b}_E \ , \quad \{\mathbf{b}_E\}_{E \in \mathcal{E}(\mathcal{M}_h)} = \mathfrak{B}_{\mathbf{U}}(\mathcal{M}_h) \ , \tag{5.64}$$

we split

$$\widetilde{\mathbf{v}}_h = \sum_{l=0}^{L} \widetilde{\mathbf{v}}_l \ , \quad \widetilde{\mathbf{v}}_l := \sum_{\substack{E \in \mathcal{E}(\mathcal{M}_h) \\ \ell(E) = l}} \alpha_E \mathbf{b}_E \ , \quad \operatorname{supp}(\widetilde{\mathbf{v}}_l) \subset \overline{\omega}_l \ . \tag{5.65}$$

The estimate $\left\|h^{-1}\widetilde{\mathbf{v}}_h\right\|_{L^2(\Omega)} \leq C \left\|\mathbf{curl}\,\mathbf{v}_h\right\|_{L^2(\Omega)}$ from Lemma 5.10 means that $\widetilde{\mathbf{v}}_h$ is "small on fine scales". Thanks to the L^2-stability (2.4) of the edge bases, this carries over to $\widetilde{\mathbf{v}}_l$:

$$
\begin{aligned}
\sum_{l=0}^{L} h_l^{-2} \left\|\widetilde{\mathbf{v}}_l\right\|_{L^2(\Omega)}^2 &\leq C \sum_{l=0}^{L} h_l^{-2} \sum_{E\in\mathcal{E}(\mathcal{M}_h),\ell(E)=l} \alpha_E^2 \left\|\mathbf{b}_E\right\|_{L^2(\Omega)}^2 \\
&\leq C \sum_{l=0}^{L} h_l^{-2} \sum_{E\in\mathcal{E}(\mathcal{M}_h),\ell(E)=l} \alpha_E^2 \left\|\mathbf{b}_E\right\|_{L^2(T_E)}^2 \\
&\leq C \sum_{l=0}^{L} h_l^{-2} \left\|\widetilde{\mathbf{v}}_h\right\|_{L^2(\Sigma_l)}^2 \leq C \left\|h^{-1}\widetilde{\mathbf{v}}_h\right\|_{L^2(\Omega)}^2 ,
\end{aligned} \tag{5.66}
$$

where $T_E \in \mathcal{M}_h$ is coarsest element adjacent to E, *cf.* (5.63), and refinement strips are defined by

$$
\Sigma_l := \omega_l \setminus \overline{\omega_{l+1}} \, , \; 0 \leq l < L, \quad \Sigma_L := \omega_L \, , \tag{5.67}
$$

see Figs. 4.1 and 4.2.

Yet, in the case of bisection refinement, $\widetilde{\mathbf{v}}_l$ may not be spanned by basis functions in $\mathfrak{B}_{\mathbf{U}}^l$, because the basis function of $\mathbf{U}(\mathcal{M}_h)$ attached to each edge on $\overline{\Sigma_l} \bigcap \overline{\omega_{l+1}}$, $0 \leq l < L$ does not belong to any $\mathfrak{B}_{\mathbf{U}}^l$!

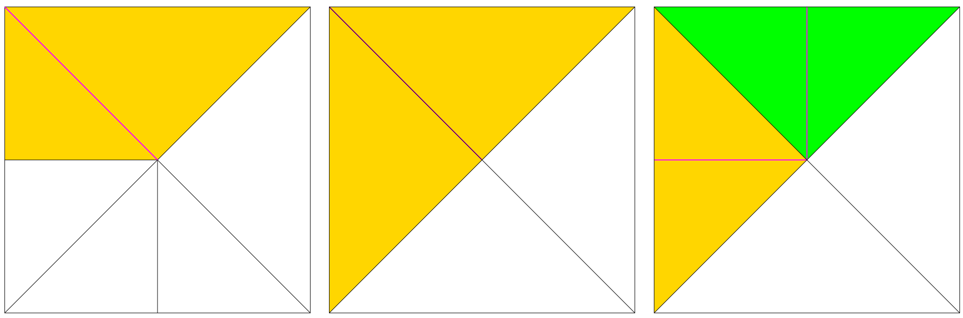

Edge E, support of basis function $\mathbf{b}_E$ | Support of $\mathbf{b}_E^l$ | Edges supporting $\mathbf{b}_{E_1}^{l+1}$, $\mathbf{b}_{E_2}^{l+1}$

FIG. 5.5. *Basis function with which* $\mathbf{b}_E$ *can be represented*

Take any $E \subset \overline{\Sigma_l} \bigcap \overline{\omega_{l+1}}$. Let $\mathbf{b}_E$, $\mathbf{b}_E^l$, and $\mathbf{b}_E^{l+1}$ be the basis functions of $\mathbf{U}(\mathcal{M}_h)$, $\mathbf{U}(\mathcal{M}_l)$, and $\mathbf{U}(\mathcal{M}_{l+1})$ associated with E, see Fig. 5.5 for a 2D illustration. Denote by $K_1, \ldots, K_n$ all elements in ω_{l+1} and $\mathcal{M}_l$ which contain E, and by $E_1, \ldots, E_m$ their new edges connecting E but not contained by the refinement edges of $K_1, \ldots, K_n$ (see Fig. 5.6). Supposing the orientations of each E_i and E point to their common endpoint, we have

$$
\mathbf{b}_E = \mathbf{b}_E^l + \frac{1}{2} \sum_{i=1}^{m} \mathbf{b}_{E_i}^{l+1} \, . \tag{5.68}
$$

This decomposition is L^2-stable with constants merely depending on shape regularity.

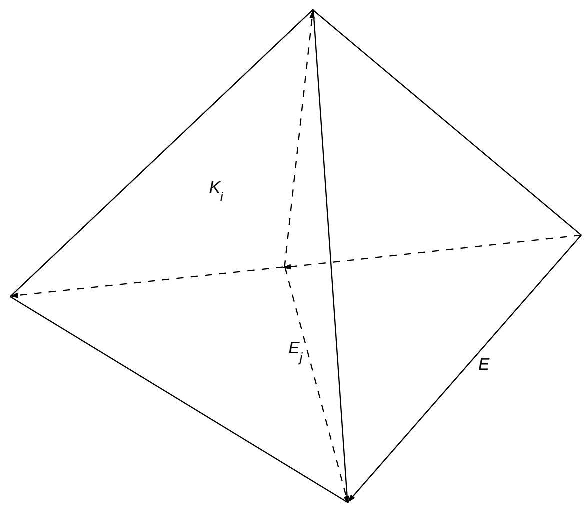

FIG. 5.6. *An edge E lies on the interface between Σ_l and ω_{l+1}.*

Since $\sum_{i=1}^m \mathbf{b}_{E_i}^{l+1} \in \mathfrak{B}_{\mathbf{U}}^{l+1}$, we may move the component of $\widetilde{\mathbf{v}}_l$ associated with this term to $\widetilde{\mathbf{v}}_{l+1}$ for any E. Then the decomposition (5.65) and the stability estimate (5.66) remain valid.

Summing up, the stability estimate (5.59) is preserved after replacing $\mathbf{\Pi}_l \mathbf{\Psi}_h$ with $\mathbf{\Pi}_l \mathbf{\Psi}_h + \widetilde{\mathbf{v}}_l \in \mathbf{U}(\mathcal{M}_l)$. ☐

Eventually, the proof of Thm. 4.2 is readily accomplished. With Lemma 5.11 at our disposal, we merely appeal to the L^2-stabilities expressed in (2.4) and (2.6) and inverse inequalities to see that all components in (5.54) can be split into local contributions of basis functions in $\mathfrak{B}_{\mathbf{U}}^l$ and $\mathfrak{B}_V^l$, respectively.

6. Quasi-orthogonality. The strengthened Cauchy-Schwartz inequality (4.7) has been established [46,49] for the standard H^1-conforming case, in [23] for the stand $\mathbf{H}(\mathrm{div})$-conforming case, and also been discussed in [24, 26] for the stand $\mathbf{H}(\mathbf{curl})$-conforming case. Here we resort the techniques in [23, §6] to establish (4.7) in the multilevel decompositions of $V(\mathcal{M}_h)$ and $\mathbf{U}(\mathcal{M}_h)$. Since $\mathfrak{B}_V^l \subset \mathfrak{B}_V(\widehat{\mathcal{M}}_l)$ and $\mathfrak{B}_{\mathbf{U}}^l \subset \mathfrak{B}_{\mathbf{U}}(\widehat{\mathcal{M}}_l)$, $l = 0, \dots, L$, we need merely show the quasi-orthogonality for multilevel splittings on globally refined meshes.

The trick is, not to consider the one-dimensional spaces spanned by individual basis functions as building blocks of the splitting (4.3), but larger aggregates. Thus, we put the nodal basis functions of $V(\widehat{\mathcal{M}}_l)$ and $\mathbf{U}(\widehat{\mathcal{M}}_l)$ into a small number of classes, such that the supports of any two basis functions in the same class do not overlap. Since the basis functions of $V(\widehat{\mathcal{M}}_l)$ and $\mathbf{U}(\widehat{\mathcal{M}}_l)$ are attached to active vertices and edges respectively, we may as well start with partitioning the vertices/edges of $\widehat{\mathcal{M}}_l$ into disjoint sets such that any two vertices/edges of the same set do not belong to the same tetrahedron. We denote these sets by $\mathcal{N}_l^i$, $i = 1, \dots, N_{\mathrm{N}}^l$ for vertices of $\widehat{\mathcal{M}}_l$ and $\mathcal{E}_l^i$, $i = 1, \dots, N_{\mathrm{E}}^l$ for edges $\widehat{\mathcal{M}}_l$ respectively. In fact, due to the uniform shape regularity of the meshes, N_{N}^l and N_{E}^l are bounded by a small constant integer independent of l. Define subspaces of $V(\widehat{\mathcal{M}}_l)$ and $\mathbf{U}(\widehat{\mathcal{M}}_l)$ by

$$V_l^i := \mathrm{Span}\left\{b_{\boldsymbol{p}},\ \boldsymbol{p} \in \mathcal{N}_l^i\right\} \quad \text{and} \quad \mathbf{U}_l^i = \mathrm{Span}\left\{\mathbf{b}_E,\ E \in \mathcal{E}_l^i\right\},$$

where $b_{\boldsymbol{p}}$ is the nodal basis function of $V(\widehat{\mathcal{M}}_l)$ attached to the vertex $\boldsymbol{p}$ and $\mathbf{b}_E$ is the nodal basis function of $\mathbf{U}(\widehat{\mathcal{M}}_l)$ attached to the edge E.

Note that the basis functions in one class are mutually orthogonal. Hence, the block relaxation (e.g. Gauss-Seidel) in (4.5) with $H_j = V_l^i$ or $\mathbf{U}_l^i$ is equivalent to the point relaxations performed on each vertex in $\mathcal{N}_l^i$ or each edge in $\mathcal{E}_l^i$. Thus, replacing the one-dimensional spaces in (4.10) and (4.11) with V_l^i and $\mathbf{U}_l^i$ does not affect on C_{stab} and C_{orth} in (4.8).

LEMMA 6.1. *Let K be an arbitrary open tetrahedron in $\mathcal{M}_m$ $(m = 0, 1, \dots, L-1)$ and $m < l \le L$. Then there exists a constant $C > 0$ only depending on the shape regularity of the meshes such that, for any $\mathbf{u}_l^i \in \mathbf{U}_l^i$, $i = 1, \dots, N_{\mathrm{E}}^l$ and $\mathbf{v}_m \in \mathbf{U}(\mathcal{M}_m)$,*

$$\mathsf{a}_{|K}(\mathbf{u}_l^i, \mathbf{v}_m) \le C \left\|\mathbf{curl}\,\mathbf{u}_l^i\right\|_{L^2(K)} \left\{ h_l \left\|\mathbf{v}_m\right\|_{L^2(K)} + \sqrt{h_l/h_m} \left\|\mathbf{curl}\,\mathbf{v}_m\right\|_{L^2(K)} \right\}. \tag{6.1}$$

Proof. Consider the basis representation of $\mathbf{u}_l^i$

$$\mathbf{u}_l^i = \sum_{E \in \mathcal{E}_l^i} \int_E \mathbf{u}_l^i \cdot \mathrm{d}\vec{s}\, \mathbf{b}_E = \mathbf{u}_{l,bd}^i + \mathbf{u}_{l,int}^i,$$

where

$$\mathbf{u}_{l,bd}^i = \sum_{E \subset \partial K, E \in \mathcal{E}_l^i} \int_E \mathbf{u}_l^i \cdot \mathrm{d}\vec{s}\, \mathbf{b}_E \quad \text{and} \quad \mathbf{u}_{l,int}^i = \sum_{E \subset K, E \in \mathcal{E}_l^i} \int_E \mathbf{u}_l^i \cdot \mathrm{d}\vec{s}\, \mathbf{b}_E.$$

Since $\mathbf{curl}\,\mathbf{v}_m$ is a constant vector in K and $\mathbf{u}_{l,int}^i \times \boldsymbol{n} = \mathbf{0}$ on ∂K, by Green's formula, it is easy to see

$$\int_K \mathbf{curl}\,\mathbf{u}_l^i \cdot \mathbf{curl}\,\mathbf{v}_m \mathrm{d}\boldsymbol{x} = \int_K \mathbf{curl}\,\mathbf{u}_{l,bd}^i \cdot \mathbf{curl}\,\mathbf{v}_m \mathrm{d}\boldsymbol{x} = \int_\Gamma \mathbf{curl}\,\mathbf{u}_{l,bd}^i \cdot \mathbf{curl}\,\mathbf{v}_m \mathrm{d}\boldsymbol{x},$$

where $\Gamma := \bigcup \{\operatorname{supp} \mathbf{b}_E :\ E \subset \partial K, E \in \mathcal{E}_l^i\}$ is a narrow strip along the boundary of K. Using the Cauchy-Schwartz inequality and noting that the basis functions in $\mathbf{U}_l^i$ are mutually orthogonal, we have

$$\begin{aligned} \int_K \mathbf{curl}\,\mathbf{u}_l^i \cdot \mathbf{curl}\,\mathbf{v}_m \mathrm{d}\boldsymbol{x} &\le \left\|\mathbf{curl}\,\mathbf{u}_{l,bd}^i\right\|_{L^2(\Gamma)} |\Gamma|^{1/2} \left|\mathbf{curl}\,\mathbf{v}_m\right| \\ &\le C \sqrt{\frac{h_l}{h_m}} \left\|\mathbf{curl}\,\mathbf{u}_l^i\right\|_{L^2(K)} |K|^{1/2} \left|\mathbf{curl}\,\mathbf{v}_m\right| \\ &= C \sqrt{\frac{h_l}{h_m}} \left\|\mathbf{curl}\,\mathbf{u}_l^i\right\|_{L^2(K)} \left\|\mathbf{curl}\,\mathbf{v}_m\right\|_{L^2(K)}, \end{aligned} \tag{6.2}$$

where C only depends on the shape regularity of the meshes.

To estimate the L^2-inner product in the bilinear form, we view the following fact

$$\|\mathbf{b}\|_{L^2(K)} \le C h_K^{1/2} \le C h_K \left\|\mathbf{curl}\,\mathbf{b}\right\|_{L^2(K)} \quad \forall\, \mathbf{b} \in \mathfrak{B}_{\mathbf{U}}(\widehat{\mathcal{M}}_l),\ K \subset \operatorname{supp} \mathbf{b},\ K \in \widehat{\mathcal{M}}_l,$$

where C only depends on the shape regularity of K. Since the basis functions of $\mathbf{U}_l^i$ are orthogonal, we have

$$\int_K \mathbf{u}_l^i \cdot \mathbf{v}_m \mathrm{d}\boldsymbol{x} \le \left\|\mathbf{u}_l^i\right\|_{L^2(K)} \left\|\mathbf{v}_m\right\|_{L^2(K)} \le C h_l \left\|\mathbf{curl}\,\mathbf{u}_l^i\right\|_{L^2(K)} \left\|\mathbf{v}_m\right\|_{L^2(K)}. \tag{6.3}$$

Now (6.1) follows from (6.2) and (6.3). $\square$

After replacing $\mathbf{U}_l^i$ with V_l^i in the proof of Lemma 6.1, similar arguments show the following Lemma:

LEMMA 6.2. *Let K be an arbitrary open tetrahedron in $\mathcal{M}_m$ $(m = 0, 1, \ldots, L-1)$ and $m < l \le L$. Then there exists a constant $C > 0$ only depending on the shape regularity of the meshes such that, for any $u_l^i \in V_l^i$, $i = 1, \ldots, N_{\mathrm{N}}^l$ and $v_m \in V(\mathcal{M}_m)$,*

$$\int_K u_l^i(\boldsymbol{x})\, v_m(\boldsymbol{x}) \mathrm{d}\boldsymbol{x} \le C\, h_l\, \left|u_l^i\right|_{H^1(K)} \|v_m\|_{L^2(K)}\,, \tag{6.4}$$

$$\int_K \operatorname{grad} u_l^i(\boldsymbol{x}) \cdot \operatorname{grad} v_m(\boldsymbol{x}) \mathrm{d}\boldsymbol{x} \le C\, \sqrt{h_l/h_m}\, \left|u_l^i\right|_{H^1(K)} |v_m|_{H^1(K)}\,. \tag{6.5}$$

As $\operatorname{grad} V(\widehat{\mathcal{M}}_l) \subset \mathbf{U}(\widehat{\mathcal{M}}_l)$ for $0 \le l \le L$, Lemmata 6.1 and 6.2 actually amount to the strengthened Cauchy-Schwartz inequality in the form (4.7) with $H_i = \mathbf{U}_l^i$ or $\operatorname{grad} V_l^i$ for the $\mathbf{H}(\mathbf{curl})$-conforming case, and $H_i = V_l^i$ for the H^1-conforming case. We denote by H_l^i the two types of lumped subspaces $\mathbf{U}_l^i$ and V_l^i.

THEOREM 6.3. *(Strengthened Cauchy-Schwartz inequality) For the decomposition of (4.10) with $H_l^i = \mathbf{U}_l^i$ and the decomposition of (4.11) with $H_l^i = V_l^i$, there exists a constant C only depending on the shape regularity of meshes such that the strengthened Cauchy-Schwartz inequality*

$$\mathsf{a}(u_l^i, v_m^j) \le C\theta^{|l-m|/2} \left\|u_l^i\right\|_A \left\|v_m^j\right\|_A \quad 0 \le i, j \le N_l,\ 0 \le l, m \le L \tag{6.6}$$

holds, where $0 < \theta < 1$ is the decrease rate of the mesh width defined in (3.3),$N_l = N_{\mathrm{E}}^l$ or N_{N}^l respectively, $\left\|u_l^i\right\|_A := \mathsf{a}(u_l^i, u_l^i)^{1/2}$, and

$$\begin{aligned} \mathsf{a}(u_l^i, v_m^j) &= (u_l^i, v_m^j)_{L^2(\Omega)} + (\mathbf{curl}\, u_l^i, \mathbf{curl}\, v_m^j)_{L^2(\Omega)} \quad \textit{if } H_l^i = \mathbf{U}_l^i, \\ \mathsf{a}(u_l^i, v_m^j) &= (u_l^i, v_m^j)_{L^2(\Omega)} + (\operatorname{grad} u_l^i, \operatorname{grad} v_m^j)_{L^2(\Omega)} \quad \textit{if } H_l^i = V_l^i. \end{aligned}$$

Proof. Without loss of generality, we assume $m \le l$ and again consider the case of uniform meshes $\widehat{\mathcal{M}}_m$ and $\widehat{\mathcal{M}}_l$. Then by Lemma 6.1 and 6.2, we have

$$\begin{aligned} \mathsf{a}(u_l^i, v_m^j) &= \sum_{K \in \widehat{\mathcal{M}}_m} \mathsf{a}_{|K}(u_l^i, v_m^j) \\ &\le C \sum_{K \in \widehat{\mathcal{M}}_m} \left|u_l^i\right|_{A,K} \left\{ h_l \left\|v_m^j\right\|_{L^2(K)} + \sqrt{h_l/h_m}\, \left|v_m^j\right|_{A,K} \right\} \\ &\le C\theta^{|l-m|/2} \sum_{K \in \widehat{\mathcal{M}}_m} \left|u_l^i\right|_{A,K} \left\|v_m^j\right\|_{A,K} \\ &\le C\theta^{|l-m|/2} \left\|u_l^i\right\|_A \left\|v_m^j\right\|_A\,, \end{aligned}$$

where $\|\cdot\|_{A,K}$ and $|\cdot|_{A,K}$ are the energy semi-norm and energy norm on K. $\square$

7. Implementation and numerical experiments. On each level l a multigrid V-cycle involves five basic operations: pre-smoothing, restriction of the equation residual to level $l-1$, prolongation of the solution from level $l-1$ to level l, correction of the solution on level l, and post-smoothing on level l.

To insure that one multigrid cycle requires only $O(N_h)$ operations with $N_h = \dim \mathbf{U}(\mathcal{M}_h)$, we rely on the so-called non-recursive implementation of the local multigrid method, *cf.* [45, 47]:

ALGORITHM 7.1. (Non-recursive local multigrid algorithm)

Given the right hand side vector f_h and the solution u_n from the last iteration, the solution u_{n+1} is defined as follows

1. Compute the residual vector

$$g_L \leftarrow f_h - \mathbb{A}_L u_n$$

2. for $l = L, \dots, 1$

   2.1. Point Gauss-Seidel relaxations associated with active edges of new elements in $\mathcal{M}_l$

$$e_l \leftarrow \mathcal{R}_l(g_l, m)$$

   2.2. Compute the restriction of the residual to $\nabla V(\mathcal{M}_l)$

$$r_l \leftarrow (I^{\mathrm{e}}_{l,\mathrm{v}})^t (g_l - \mathbb{A}_l e_l)$$

   2.3. Point Gauss-Seidel relaxations associated with active vertices of new elements in $\mathcal{M}_l$

$$\widetilde{e}_l \leftarrow \mathcal{S}_l(r_l, m)$$

   2.4. Prolongate $\widetilde{e}_l$ and correct e_l

$$e_l \leftarrow e_l + I^{\mathrm{e}}_{l,\mathrm{v}} \widetilde{e}_l$$

   2.5. Compute the restriction of the residual vector

$$g_{l-1} \leftarrow \left(I^l_{l-1}\right)^t (g_l - \mathbb{A}_l e_l)$$

   endfor

3. Exact solution of the error equation on $\mathcal{M}_0$

$$e_0 \leftarrow \mathbb{A}_0^{-1} g_0$$

4. for $l = 1, \dots, L$

   4.1. Correct e_l by the error from level $l-1$

$$e_l \leftarrow e_l + I^l_{l-1} e_{l-1}$$

   4.2. Post-smoothing: point Gauss-Seidel relaxations associated with active edges of new elements in $\mathcal{M}_l$

$$e_l \leftarrow e_l + \mathcal{R}_l(g_l - \mathbb{A}_l e_l, m)$$

   4.3. Compute the restriction of the residual to $\nabla V(\mathcal{M}_l)$

$$r_l \leftarrow (I^{\mathrm{e}}_{l,\mathrm{v}})^t (g_l - \mathbb{A}_l e_l)$$

4.4. Post-smoothing: point Gauss-Seidel relaxations associated with active vertices of new elements in $\mathcal{M}_l$

$$\widetilde{e}_l \leftarrow \mathcal{S}_l(r_l, m)$$

4.5. Prolongate $\widetilde{e}_l$ and correct e_l

$$e_l \leftarrow e_l + I^{\mathrm{e}}_{l,\mathrm{v}} \widetilde{e}_l$$

endfor

5. Correct the solution

$$u_{n+1} \leftarrow u_n + e_L$$

In Algorithm 7.1, $\mathbb{A}_l$ is the stiffness matrix of the discrete problem (2.3), $\mathcal{R}_l$ is the local Gauss-Seidel relaxation operator for (2.3), which only targets active edges of new elements in $\mathcal{M}_l$. Further, $\mathcal{S}_l$ is the local Gauss-Seidel relaxation operator related to the $V(\mathcal{M}_l)$-Galerkin matrix for (1.4). Again, it is restricted to active vertices of new elements in $\mathcal{M}_l$. The integer m is the number of Gauss-Seidel relaxations (always set to $m = 1$ in the numerical experiments reported below). Further, I^l_{l-1} is the matrix representation of the embedding operation $\mathbf{U}(\mathcal{M}_l) \mapsto \mathbf{U}(\mathcal{M}_{l+1})$, and the edge-vertex incidence matrix $I^{\mathrm{e}}_{l,\mathrm{v}}$ describes the embedding $\operatorname{grad} V(\mathcal{M}_l) \mapsto \mathbf{U}(\mathcal{M}_l)$. A superscript t tags transpose matrices.

To explain Algorithm 7.1, we denote by $\mathcal{E}^{\mathrm{new}}_l = \{E^l_1, \ldots, E^l_{N_l}\}$ the set of edges of new elements and by $\mathcal{N}^{\mathrm{new}}_l = \{\boldsymbol{p}^l_1, \ldots, \boldsymbol{p}^l_{M_l}\}$ the set of vertices of new elements in $\mathcal{M}_l$ for convenience.

In steps 2.1 and 4.2, $x \leftarrow \mathcal{R}_l(y, 1)$ is equivalent to

$$x(E) \leftarrow \frac{y(E)}{\mathsf{a}(\mathbf{b}_E, \mathbf{b}_E)} \quad \forall\, E \in \mathcal{E}^{\mathrm{new}}_l,$$

where $x(E)$ is the component of x associated with E. In step 2.3 and 4.4, $x \leftarrow \mathcal{S}_l(y, 1)$ is equivalent to

$$x(\boldsymbol{p}) \leftarrow \frac{y(\boldsymbol{p})}{(\operatorname{grad} b_{\boldsymbol{p}}, \operatorname{grad} b_{\boldsymbol{p}})_{L^2(\Omega)}} \quad \forall\, \boldsymbol{p} \in \mathcal{N}^{\mathrm{new}}_l,$$

where $x(\boldsymbol{p})$ is the component of x associated with $\boldsymbol{p}$. Thus the total number of operations of these steps is $O(N_l + M_l) = O(N_l)$.

The concrete implementation of prolongation and restriction operators is as follows. In step 4.1, let $K \in \mathcal{M}_{l-1} \setminus \mathcal{M}_l$ and define

$$\mathbf{e}_{l-1} = \sum_{E \subset \partial K, E \in \mathcal{E}(\mathcal{M}_{l-1})} e_{l-1}(E)\, \mathbf{b}_E \quad \text{in } K.$$

For any $K' \in \mathcal{M}_l$ and $K' \subset K$, we have

$$\left(I^l_{l-1} e_{l-1}\right)(E') = \int_{E'} \mathbf{e}_{l-1} \cdot \mathrm{d}\vec{s} \quad \forall\, E' \subset \partial K',\ E' \in \mathcal{E}(\mathcal{M}_l).$$

Similarly, steps 2.4 and 4.5 are realized as follows:

$$\widetilde{\mathbf{e}}_l = \sum_{\boldsymbol{p} \in \partial K,\, \boldsymbol{p} \in \mathcal{N}(\mathcal{M}_l)} \widetilde{e}_l(\boldsymbol{p}) \operatorname{grad} b_{\boldsymbol{p}} \quad \text{in } K \in \mathcal{M}_l \setminus \mathcal{M}_{l-1}.$$

For any $K \in \mathcal{M}_l \setminus \mathcal{M}_{l-1}$, we have

$$\left(I^{\mathrm{e}}_{l,\mathrm{v}}\widetilde{e}_l\right)(E) = \int_E \widetilde{\mathbf{e}}_l \cdot \mathrm{d}\vec{s} \quad \forall\, E \subset \partial K,\ E \in \mathcal{E}(\mathcal{M}_l).$$

Clearly, the prolongation processes only involve operations on new elements in $\mathcal{M}_l$ and thus the total number of computations is also $O(N_l)$. The restriction matrices in steps 2.2, 4.3, and 2.5 are the transposes of the corresponding prolongation matrices, and, thus, only involve operations on new elements. The total number of computations required for the transfer operations on level l is of order $O(N_l)$.

Now we discuss how to compute the product $\mathbb{A}_l e_l$ in step 2.2, 2.5, 4.2, and 4.3 efficiently. Since $\mathcal{R}_l$ only involves the operations on $\mathcal{E}_l^{\mathrm{new}}$, e_l in step 2.2 only have nonzero components associated with the edges in $\mathcal{E}_l^{\mathrm{new}}$. Furthermore, since $(I^l_{l-1})^t$ only affects $\mathcal{E}_l^{\mathrm{new}}$, we may compute $\xi_l = \mathbb{A}_l e_l$ in step 2.2 as follows:

Algorithm 7.2.

```
for i = 1,...,N_l
    ξ_l(E_i) = 0
    for j = 1,...,N_l
        ξ_l(E_i) ← ξ(E_i) + A_l(E_i, E_j) × e_l(E_j)
    endfor
endfor
```

Algorithm 7.2 clearly needs only $O(N_l)$ operations. A further examination of the algorithm reveals that all that is needed is a $N_l \times N_l$ sub-block of the stiffness matrix $\mathbb{A}_l$. This can be computed in $O(N_l)$ operations. As for the computation of $\xi = \mathbb{A}_l e_l$ in steps 2.5, 4.2, and 4.3, note that $(I^l_{l-1})^t$ in step 2.5, $(I^{\mathrm{e}}_{l,\mathrm{v}})^t$ in step 4.3, and $\mathcal{R}_l$ in step 4.2 only involve new elements; everything can be done along the lines of Algorithm 7.2.

The last computation concerns the corrections in step 2.4, 4.1, 4.2, and 4.5. Since all other operations on the l-th level only involve new elements, each degree of freedom $e_l(E)$, $E \in \mathcal{E}(\mathcal{M}_l) \setminus \mathcal{E}_l^{\mathrm{new}}$ remains unchanged. Thus, asymptotically, $O(N_l)$ computations are sufficient to add the correction.

The number of computations in step 1 and 5 is at most $O(N_h)$ and the effort for step 3 is negligible. Finally, we obtain the total number of operations in one step of local multigrid iteration by summing up the computations on all levels:

$$O(N_h) + \sum_{l=1}^{L} O(N_l) = O(N_h) + O\left(\sum_{l=1}^{L} N_l\right) = O(N_h).$$

We conclude that the non-recursive implementation of the local multigrid method is optimal in terms of the amount of computations in each iteration.

In the ensuing numerical experiments the implementation of adaptive mesh refinement was based on the adaptive finite element package ALBERT [37], which uses the bisection strategy of [29], see Sect. 3.

Let $\mathcal{M}_0$ be an initial mesh satisfying the two assumptions (A1) and (A2) in [29, P. 282], the adaptive mesh refinements are governed by a residual based a posteriori error estimator: given a finite element approximation $\mathbf{u}_h \in \mathbf{U}(\mathcal{M}_h)$, for any $T \in \mathcal{M}_h$ the estimator is given by

$$\eta_T^2 := h_T^2 \|\mathbf{f} - \mathbf{u}_h\|^2_{\mathbf{H}(\mathrm{div},T)} + \frac{h_T}{2} \sum_{F \subset \partial T} \Big\{ \|[\mathbf{u}_h]_F\|^2_{0,F} + \|[\mathbf{curl}\,\mathbf{u}_h \times \boldsymbol{\nu}]_F\|^2_{0,F} \Big\},$$

where F is a face of T, $\boldsymbol{\nu}$ is the unit normal of F, and $[\mathbf{u}_h]_F$ is the jump of $\mathbf{u}_h$ across F. The global a posteriori error estimate and the maximal estimated element error on $\mathcal{M}_h$ are defined by

$$\eta_h := \left(\sum_{T\in\mathcal{M}_h} \eta_T^2 \right)^{1/2}, \qquad \eta_{\max} = \max_{T\in\mathcal{M}_h} \eta_T. \tag{7.1}$$

Using η_h and $\eta_{\max}$, we use [14, Algorithm 5.1] to mark and refine $\mathcal{M}_h$ adaptively.

In the following, we report two numerical experiments to demonstrate the competitive behavior of the local multigrid method and to validate our convergence theory.

EXAMPLE 7.1. *We consider the Maxwell equation on the three-dimensional "L-shaped" domain* $\Omega = (-1,\ 1)^3 \setminus \{(0,\ 1)\times(-1,\ 0)\times(-1,\ 1)\}$. *The Dirichlet boundary condition and the righthand side* $\mathbf{f}$ *are chosen so that the exact solution is*

$$\mathbf{u} := \nabla\left\{ r^{1/2}\sin(\phi/2) \right\}$$

in cylindrical coordinates (r,ϕ,z).

Table 7.1 shows the numbers of multigrid iterations required to reduce the initial residual by a factor 10^{-8} on different levels. We observe that the multigrid algorithm converges in almost the same small number of steps, though the number of elements varies from 156 to 100,420.

TABLE 7.1
The number of adaptive iterations $N_{\rm it}$, the number of elements $N_{\rm el}$, the number of multigrid iterations N_{itrs} required to reduce the initial residual by a factor 10^{-8}, the relative error between the true solution $\mathbf{u}$ and the discrete solution $\mathbf{u}_h$: $E_{\rm rel} = \|\mathbf{u}-\mathbf{u}_h\|_{\mathbf{H}(\mathbf{curl},\Omega)} \,/\, \|\mathbf{u}\|_{\mathbf{H}(\mathbf{curl},\Omega)}$ (Example 7.1).

$N_{\rm it}$	2	5	10	15	20	25	30	35
$N_{\rm el}$	156	388	1,900	4,356	9608	19,424	48,088	100,420
$E_{\rm rel}$	0.4510	0.3437	0.2456	0.1919	0.1600	0.1350	0.1094	0.0915
N_{itrs}	11	21	19	19	19	19	19	19

Fig. 7.1 plots the CPU time versus the number of degrees of freedom on different adaptive meshes. It shows that the CPU time of solving the algebraic system increases roughly linearly with respect to the number of elements.

Fig. 7.2 depicts a locally refined mesh of 100,420 elements created by the adaptive finite element algorithm.

EXAMPLE 7.2. *This example uses the same solution as Example 7.1*

$$\mathbf{u} := \nabla\left\{ r^{1/2}\sin(\phi/2) \right\}$$

in cylindrical coordinates (r,ϕ,z). *But the computational domain is changed to a three-dimensional non-Lipschitz domain with an inner crack-type boundary, which is defined by*

$$\Omega = (-1,\ 1)^3 \setminus \{(x,0,z):\ 0 \le x < 1,\ -1 < z < 1\}.$$

The Dirichlet boundary condition and the source function $\mathbf{f}$ *are the same as above.*

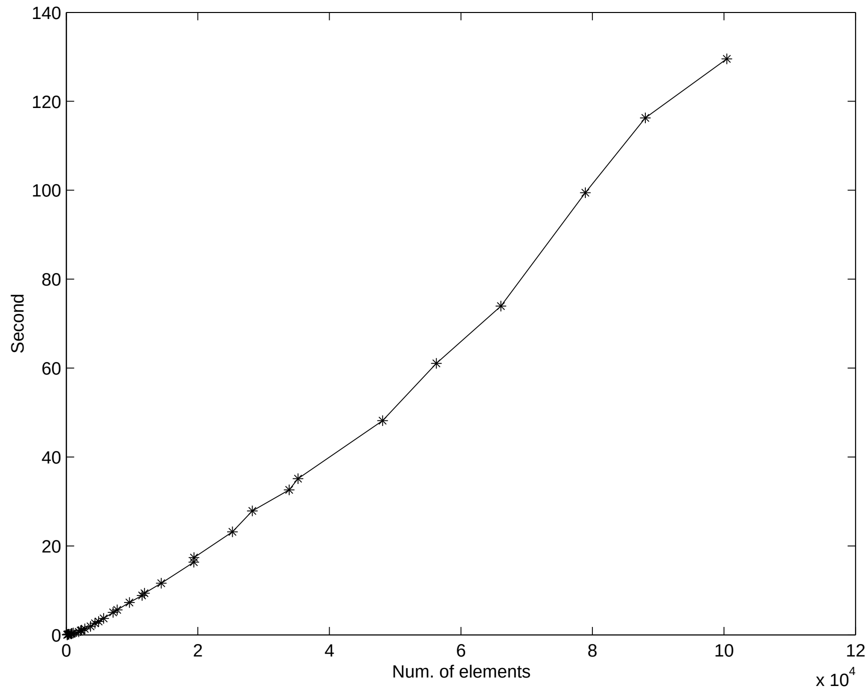

FIG. 7.1. *CPU time for solving the algebraic system by multigrid method(Example 7.1).*

TABLE 7.2

The number of adaptive iterations N_{it}, the number of elements N_{el}, the number of multigrid iterations N_{itrs} required to reduce the initial residual by a factor 10^{-8}, the relative error between the true solution $\mathbf{u}$ and the discrete solution $\mathbf{u}_h$: $E_{\mathrm{rel}} = \|\mathbf{u}-\mathbf{u}_h\|_{\mathbf{H}(\mathbf{curl},\Omega)} / \|\mathbf{u}\|_{\mathbf{H}(\mathbf{curl},\Omega)}$ (Example 7.2).

N_{it}	2	5	10	15	20	25	30	33
N_{el}	128	404	1,236	3,416	12,420	29,428	81,508	135,876
E_{rel}	0.4616	0.3762	0.2992	0.2347	0.1752	0.1394	0.1095	0.0958
N_{itrs}	14	30	25	26	26	27	27	27

Table 7.2 records the numbers of multigrid iterations required to reduce the initial residual by a factor 10^{-8} on different levels. We observe that the multigrid algorithm converges in less than 30 steps, with the number of elements soaring from 128 to 135,876.

Fig. 7.3 shows the CPU time versus the number of degrees of freedom on different adaptive meshes. Obviously, the CPU time for solving the algebraic system increases nearly linearly with respect to the number of elements.

Fig. 7.4 displays a locally refined mesh of 135,876 elements using adaptive finite element algorithm. In addition, the restriction of the mesh to the cross-section $\{y = 0\}$, which contains the inner boundary, is drawn. This reveals strong local refinement.

This experiment bears out that the local multigrid is also efficient for the problems in non-Lipschitz doamins, which are outside the scope of our theory.

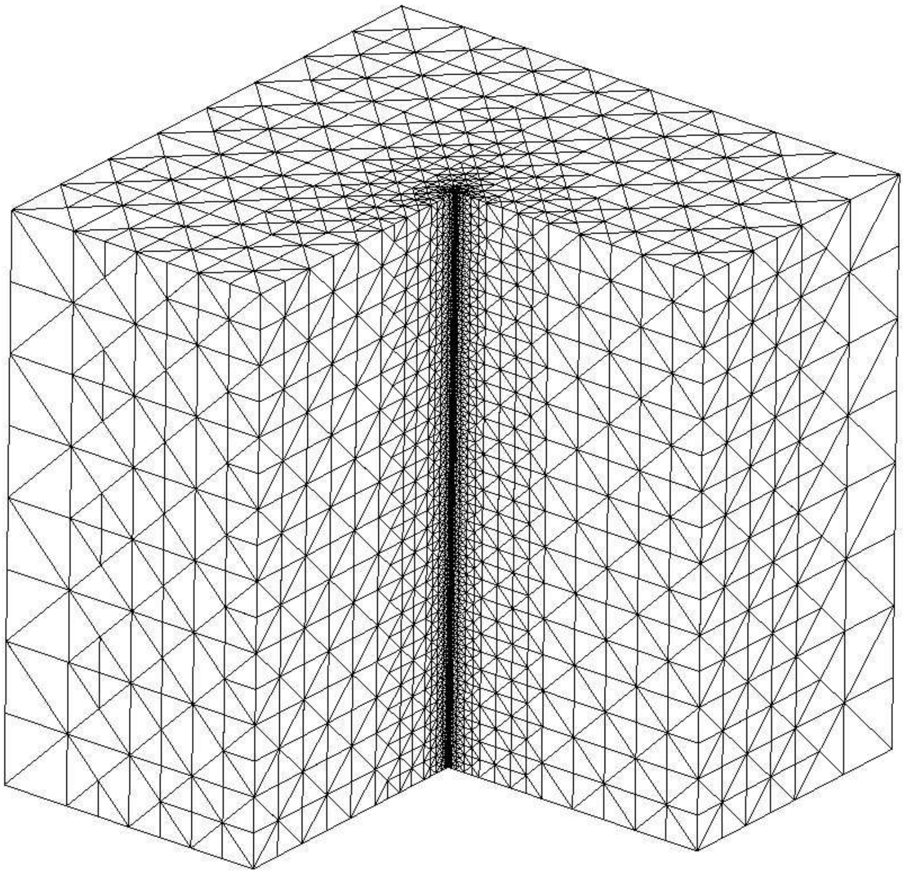

FIG. 7.2. *A locally refined mesh of 100,420 elements (Example 7.1).*

Acknowledgement. The authors would like to thank Dr. L. Wang of Computer Network Information Center, Prof. Z. Chen and Prof. L. Zhang of the Institute of Computational Mathematics, Chinese Academy of Sciences, for their support in the implementation of the local multigrid method.

REFERENCES

[1] M. AINSWORTH AND W. MCLEAN, *Multilevel diagonal scaling preconditioners for boundary element equations on locally refined meshes*, Numer. Math., 93 (2003), pp. 387–413.

[2] D. ARNOLD, R. FALK, AND R. WINTHER, *Multigrid in* $H(\mathrm{div})$ *and* $H(\mathbf{curl})$, Numer. Math., 85 (2000), pp. 175–195.

[3] ———, *Finite element exterior calculus, homological techniques, and applications*, Acta Numerica, 15 (2006), pp. 1–155.

[4] D. BAI AND A. BRANDT, *Local mesh refinement multilevel techniques*, SIAM J. Sci. Stat. Comput., 8 (1987), pp. 109–134.

[5] E. BÄNSCH, *Local mesh refinement in 2 and 3 dimensions*, IMPACT Comput. Sci. Engrg., 3 (1991), pp. 181–191.

[6] R. BECK, P. DEUFLHARD, R. HIPTMAIR, R. HOPPE, AND B. WOHLMUTH, *Adaptive multilevel methods for edge element discretizations of Maxwell's equations*, Surveys on Mathematics for Industry, 8 (1998), pp. 271–312.

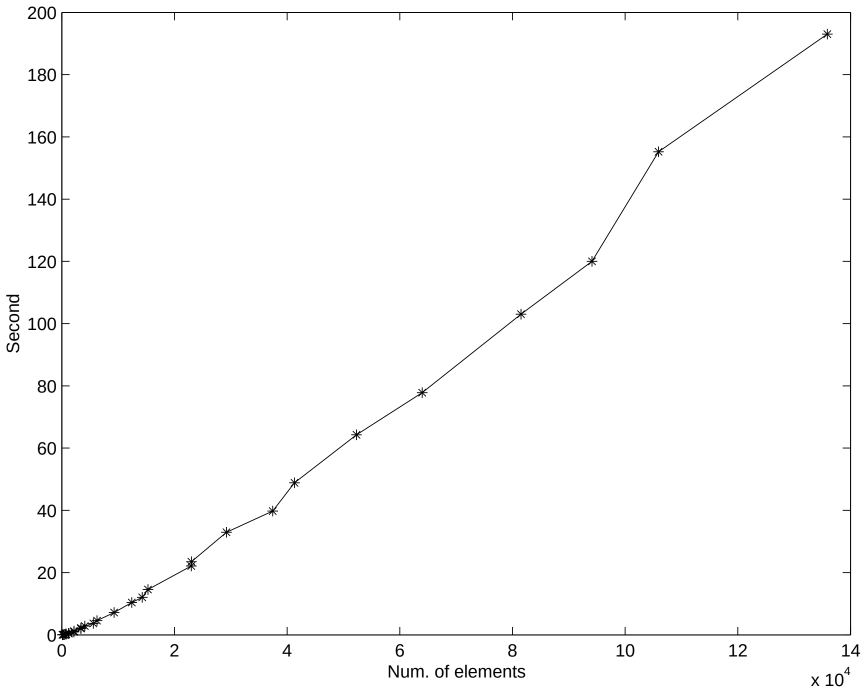

Fig. 7.3. *CPU time for solving the algebraic system by multigrid method(Example 7.2).*

[7] R. Beck, B. Erdmann, and R. Roitzsch, *KASKADE 3.0. An object-oriented adaptive finite element code*, Tech. Rep. TR 95-4, ZIB, Berlin, Germany, June 1995.

[8] J. Bey, *Tetrahedral grid refinement*, Computing, 55 (1995), pp. 355–378.

[9] F. Bornemann and H. Yserentant, *A basic norm equivalence for the theory of multilevel methods*, Numer. Math., 64 (1993), pp. 455–476.

[10] A. Bossavit, *Whitney forms: A class of finite elements for three-dimensional computations in electromagnetism*, IEE Proc. A, 135 (1988), pp. 493–500.

[11] J. Bramble and J. Pasciak, *New estimates for multilevel methods including the V–cycle*, Math. Comp., 60 (1993), pp. 447–471.

[12] J. Bramble, J. Pasciak, J. Wang, and J. Xu, *Convergence estimates for product iterative methods with applications to domain decomposition*, Math. Comp., 57 (1991), pp. 1–21.

[13] A. Buffa, M. Costabel, and D. Sheen, *On traces for* $\mathbf{H}(\mathbf{curl},\Omega)$ *in Lipschitz domains*, J. Math. Anal. Appl., 276 (2002), pp. 845–867.

[14] Z.-M. Chen, L. Wang, and W.-Y. Zheng, *An adaptive multilevel method for time-harmonic maxwell equations with singularities*, SIAM J. Sci. Comp., (2006). To appear.

[15] P. Ciarlet, *The Finite Element Method for Elliptic Problems*, vol. 4 of Studies in Mathematics and its Applications, North-Holland, Amsterdam, 1978.

[16] M. Clemens, S. Feigh, and T. Weiland, *Geometric multigrid algorithms using the conformal finite integration technique*, IEEE Trans. Magnetics, 40 (2004), pp. 1065–1068.

[17] P. Clément, *Approximation by finite element functions using local regularization*, RAIRO Anal. Numér., 2 (1975), pp. 77–84.

[18] M. Costabel and M. Dauge, *Singularities of electromagnetic fields in polyhedral domains*, Arch. Rational Mech. Anal., 151 (2000), pp. 221–276.

[19] M. Costabel, M. Dauge, and S. Nicaise, *Singularities of eddy current problems*, ESAIM: Mathematical Modelling and Numerical Analysis, 37 (2003), pp. 807–831.

[20] V. Girault and P. Raviart, *Finite element methods for Navier–Stokes equations*, Springer, Berlin, 1986.

[21] J. Gopalakrishnan, J. Pasciak, and L. Demkowicz, *Analysis of a multigrid algorithm for time harmonic maxwell equations*, SIAM J. Numer. Anal., 42 (2003), pp. 90–108.

[22] P. Grisvard, *Elliptic Problems in Nonsmooth Domains*, Pitman, Boston, 1985.

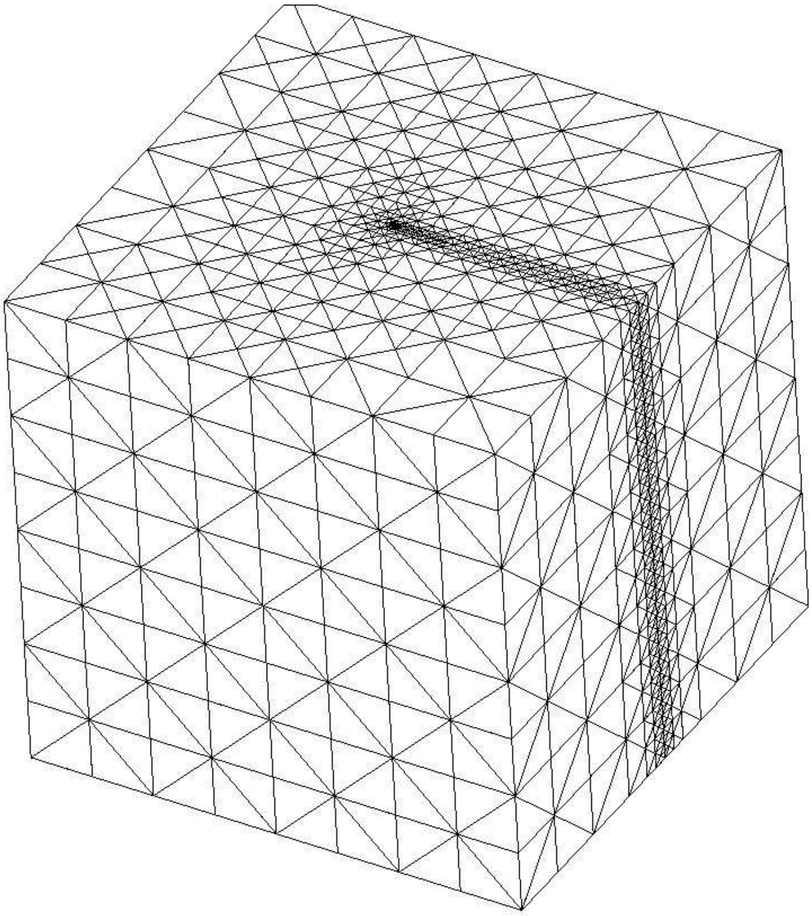

FIG. 7.4. *A locally refined mesh of 135,876 elements (Example 7.2).*

[23] R. HIPTMAIR, *Multigrid method for Maxwell's equations*, Tech. Rep. 374, Institut für Mathematik, Universität Augsburg, 1997. USE HIP 99.

[24] ———, *Multigrid method for Maxwell's equations*, SIAM J. Numer. Anal., 36 (1999), pp. 204–225.

[25] ———, *Finite elements in computational electromagnetism*, Acta Numerica, 11 (2002), pp. 237–339.

[26] ———, *Analysis of multilevel methods for eddy current problems*, Math. Comp., 72 (2003), pp. 1281–1303.

[27] R. HIPTMAIR, G. WIDMER, AND J. ZOU, *Auxiliary space preconditioning in* $\mathbf{H}_0(\mathbf{curl}, \Omega)$, Numer. Math., 103 (2006), pp. 435–459.

[28] R. HIPTMAIR AND J. XU, *Nodal auxiliary space preconditioning in H(curl) and H(div) spaces*, Report 2006-09, SAM, ETH Zürich, Zürich, Switzerland, 2006.

[29] I. KOSSACZKÝ, *A recursive approach to local mesh refinement in two and three dimensions*, J. Comput. Appl. Math., 55 (1994), pp. 275–288.

[30] J. LIONS AND F. MAGENES, *Nonhomogeneous boundary value problems and applications*, Springer–Verlag, Berlin, 1972.

[31] J. MAUBACH, *Local bisection refinement for n–simplicial grids generated by reflection*, SIAM J. Sci. Stat. Comp., 16 (1995), pp. 210–227.

[32] W. MITCHELL, *Optimal multilevel iterative methods for adaptive grids*, SIAM J. Sci. Stat. Comput, 13 (1992), pp. 146–167.

[33] J. NÉDÉLEC, *Mixed finite elements in* $\mathbb{R}^3$, Numer. Math., 35 (1980), pp. 315–341.

[34] P. OSWALD, *On function spaces related to the finite element approximation theory*, Z. Anal.

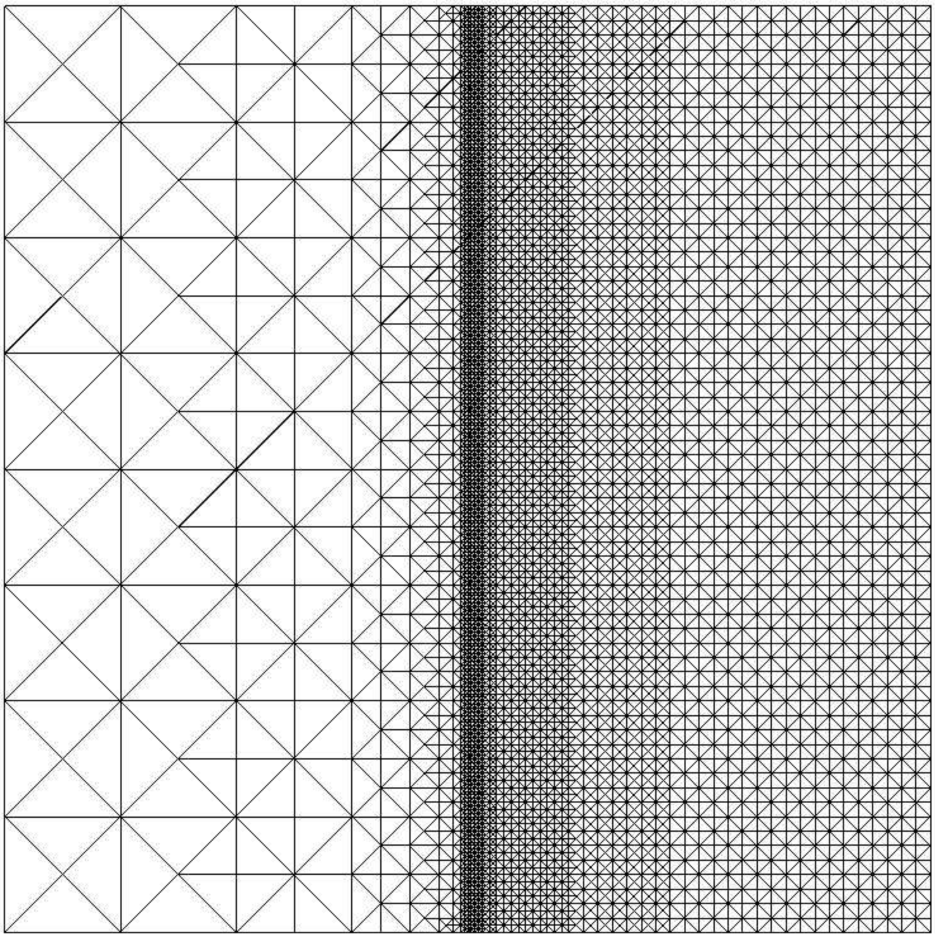

Fig. 7.5. *The mesh on the cross* $\{x_2 = 0\}$ *of the domain* Ω (*Example 7.1*).

Anwendungen, 9 (1990), pp. 43–64.
[35] ———, *Multilevel finite element approximation*, Teubner Skripten zur Numerik, B.G. Teubner, Stuttgart, 1994.
[36] J. Pasciak and J. Zhao, *Overlapping Schwarz methods in H(curl) on polyhedral domains*, J. Numer. Math., 10 (2002), pp. 221–234.
[37] A. Schmidt and K. Siebert, *ALBERT – An adaptive hierarchical finite element toolbox.* Website. ALBERTA is available online from http://www.alberta-fem.de.
[38] A. Schmidt and K. Siebert, *Design of Adaptive Finite Element Software: The Finite Element Toolbox ALBERTA*, Lecture Notes in Computational Science and Engineering, Springer, Heidelberg, 2005.
[39] J. Schöberl, *Commuting quasi-interpolation operators for mixed finite elements*, Preprint ISC-01-10-MATH, Texas A&M University, College Station, TX, 2001.
[40] L. R. Scott and Z. Zhang, *Finite element interpolation of nonsmooth functions satisfying boundary conditions*, Math. Comp., 54 (1990), pp. 483–493.
[41] O. Sterz, A. Hauser, and G. Wittum, *Adaptive local multigrid methods for solving time-harmonic eddy current problems*, IEEE Trans. Magnetics, 42 (2006), pp. 309–318.
[42] R. Stevenson, *Optimality of a standard adaptive finite element method*, Foundations of Com-

putational Mathematics, (2006). DOI 10.1007/s10208-005-0183-0.
[43] B. Weiss and O. Biro, *Multigrid for time-harmonic 3-d eddy-current analysis with edge elements*, IEEE Trans. Magnetics, 41 (2005), pp. 1712–1715.
[44] H. Whitney, *Geometric Integration Theory*, Princeton University Press, Princeton, 1957.
[45] H.-J. Wu and Z.-M. Chen, *Uniform convergence of multigrid v-cycle on adaptively refined finite element meshes for second order elliptic problems*, Science in China: Series A Mathematics, 49 (2006), p. 1C28.
[46] J. Xu, *Iterative methods by space decomposition and subspace correction*, SIAM Review, 34 (1992), pp. 581–613.
[47] ———, *An introduction to multilevel methods*, in Wavelets, Multilevel Methods and Elliptic PDEs, M. Ainsworth, K. Levesley, M. Marletta, and W. Light, eds., Numerical Mathematics and Scientific Computation, Clarendon Press, Oxford, 1997, pp. 213–301.
[48] J. Xu and L. Zikatanov, *The method of alternating projections and the method of subspace corrections in Hilbert space*, Report AM 223, Department of Mathematics, PennState University, College Park, PA, June 2000. Submitted.
[49] H. Yserentant, *On the multi–level splitting of finite element spaces*, Numer. Math., 58 (1986), pp. 379–412.
[50] ———, *Old and new convergence proofs for multigrid methods*, Acta Numerica, (1993), pp. 285–326.

Appendix A. Notations.

$\boldsymbol{H}(\mathbf{curl},\Omega)$	: Sobolev space of square integrable vector fields on $\Omega\subset\mathbb{R}^3$ with square integrable **curl**
$\boldsymbol{H}_{\Gamma_D}(\mathbf{curl},\Omega)$	: vector fields in $\boldsymbol{H}(\mathbf{curl},\Omega)$ with vanishing tangential components on $\Gamma_D\subset\partial\Omega$
$\mathcal{M}$, $\mathcal{T}$	: tetrahedral finite element meshes, may contain hanging nodes
$\rho_K,\rho_{\mathcal{M}}$	: shape regularity measures
h	: – local meshwidth function for a finite element mesh – (as subscript) tag for finite element functions
$\mathbf{U}(\mathcal{M})$	: lowest order edge element space on $\mathcal{M}$
$\mathbf{b}_E$	: nodal basis function of $\mathbf{U}(\mathcal{M})$ associated with edge E
$V(\mathcal{M})$	: space of continuous piecewise linear functions on $\mathcal{M}$
$b_{\boldsymbol{p}}$	: nodal basis function of $V(\mathcal{M})$ ("tent function") associated with vertex $\boldsymbol{p}$
$\mathfrak{B}_X(\mathcal{M})$	: set of nodal basis functions for finite element space X on mesh $\mathcal{M}$
$\mathbf{\Pi}_h$	: nodal edge interpolation operator onto $\mathbf{U}(\mathcal{M})$
$\mathcal{I}_h$	: piecewise linar interpolation
$\mathbb{P}_p$	: space of 3-variate polynomials of total degree $\leq p$
ω_l	: refinement zone, see (4.1)
Σ_l	: refinement strip, see (5.67)
$\mathfrak{B}^l_V$, $\mathfrak{B}^l_{\mathbf{U}}$	: sets of basis functions supported inside refinement zones, see (4.9)
Q_h	: quasi-interpolation operator, Def. 5.1